A STUDY OF VASCULAR TRANSPORT OF PLANT EXOGENOUS PROTEINS IN *NICOTIANA BENTHAMIANA* AND *BRASSICA OLERACEA* USING FLUORESCENCE AND MEGNETIC RESONANCE IMAGING TECHNOLOGY

By

CHENXING NIU

Bachelor of Science in Plant Protection

China Agricultural University

Beijing, China

2008

Submitted to the Faculty of the
Graduate College of the
Oklahoma State University
in partial fulfillment of
the requirements for
the Degree of
MASTER OF SCIENCE
July, 2011

A STUDY OF VASCULAR TRANSPORT OF PLANT EXOGENOUS PROTEINS IN *NICOTIANA BENTHAMIANA* AND *BRASSICA OLERACEA* USING FLUORESCENCE AND MEGNETIC RESONANCE IMAGING TECHNOLOGY

Thesis Approved:

Dr. Jeanmarie Verchot

Thesis Adviser

Dr. Francisco Ochoa-Corona

Dr. Astri Wayadande

Dr. Stephen Marek

Dr. Mark E. Payton

Dean of the Graduate College

ACKNOWLEDGEMENTS

I would like to express my sincere gratitude to my major advisor, Dr. Jeanmarie Verchot. She created an environment where I grew from a student to a scientist. Her supervision, inspiration and encouragement played important role on my degree. I would also like to thank my committee members, Dr. Francisco Ochoa-Corona, Dr. Astri Wayadande and Dr. Stephen Marek. They are always willing to give suggestion and help. Their patient explanation, thoughtful comments and encouragement ensured completion of my study. I also wish to acknowledge and thank Dr. Phillip Mulder, Jr., Dr. Kristopher Giles, Dr. Robert Hunger as well as lab members, Dr. Changming Ye and Asitha Silva, their patient, kind guidance and encouragement support me overcome the difficulties and verdancy as an international student. My gratitude also extends to all department members and members in Dr. Rheal Towner Lab (Oklahoma Medical Research Foundation) who supply a firm foundation and thrill environment during my study. I am inspired by the passion from the way they speak, the gesture they make, the smile on their faces and the attitude when they eager to find the answers for questions. I cannot express enough gratitude to my family for allowing me to find something I am truly passionate about. I am thankful that have this fortune to have such wonderful people in my life.

TABLE OF CONTENTS

Chapter Page

LIST OF TABLES

LIST OF FIGURES

Figure Page

CHAPTER I

CHAPTER II

Figure Page

CHAPTER I

INTRODUCTION AND LITERATURE REVIEW

The plant vasculature is composed of xylem and phloem

The xylem and phloem comprise the plant vasculature and function for transporting water, photoassimilates, proteins, nucleic acids, and other micronutrients to various organs of the plant. The xylem transports water and minerals and is composed of tracheary elements (tracheids, vessel elements), xylem parenchyma as well as fibers. Tracheids are elongated, spindle-shaped cells that are connected to form vertical strands, which are present in angiosperms, gymnosperms and ferns (Taiz and Zeiger, 2006). Vessel elements are shorter and wider than tracheids, and occur in angiosperms as well as a small group of gymnosperms called Gnetales (Taiz and Zeiger, 2006). Water is transported via the xylem from the roots into aerial parts of the plant. Water moves into the root cortex and is driven into the xylem. Negative pressure at the top of the plant can "pull" the water upward from the root creating "bulk flow" (mass flow) movement. The cohesion-tension theory is used to explain water conductance in the xylem. It is the cohesion of water molecules that enables capillary action driving upward movement of water and molecules contained in the water (Taiz and Zeiger, 2006).

The three cellular components of the phloem are: a) sieve elements (SEs); b) companion cells (CCs), and c) parenchyma cells. In angiosperms, sieve elements form vertical structures known as sieve tubes which carry photoassimilates and macromolecules throughout the plant (Taiz and Zeiger, 2006). Only the SEs are directly involved in sap translocation. In angiosperms, SEs develop from intact cells, which lose most of their metabolic activity and organelles, such as nuclei, tonoplasts, microtubules, ribosomes and Golgi bodies, during maturation. SEs are highly specialized for assimilate translocation (Taiz and Zeiger, 2006). CCs contain extraordinarily dense cytoplasm containing numerous mitochondria, plastids and free ribosomes, which function to provide nutrients to the SEs and funnel macromolecules for transport into the sieve tubes (Taiz and Zeiger, 2006). Throughout the phloem, photoassimilates, proteins, and other macromolecules are translocated to various destinations in the plant.

Phloem transport occurs in a source-to-sink direction, meaning that transport initiates at the mature leaves which are the main source of macromolecule synthesis, and move towards younger developing leaves or organs (sink tissues) that are not actively synthesizing these compounds. The delivery of macromolecules to sink tissues is necessary for their growth, development and defense against environmental stresses. The most abundant component of phloem sap are carbohydrates, especially sucrose (Hall and Baker, 1972). The pressure-flow model describes the mass flow of sap driven by an osmotically generated pressure gradient between source and sink tissues (Taiz and Zeiger, 2006). Movement of carbohydrates from CCs into the SEs in source tissues lowers the water potential. This causes water to enter from the xylem, creating a pressure that drives movement of sap in the direction of sink tissues. Phloem unloading in sink

tissues causes a decrease of sugar concentration and high water potential. Water cycles from the phloem to xylem, maintaining the appropriate pressure in the sink to enable transport of macromolecules from the source tissues (Taiz and Zeiger, 2006).

The SE- CC complex regulates phloem loading and transport. These cells are connected by plasmodesmata connections that enable the exchange of macromolecules (Oparka and Turgeon, 1999; Taiz and Zeiger, 2006). CCs provide nutritional support for SEs and control the movement of most macromolecules into the SEs. While movement of sugar from the mesophyll to the bundle sheath cell is a short symplastic route, phloem loading in the SE-CC complex occurs by both apoplastic and symplastic routes. Sugars first enter the apoplast near the SE-CC complex and then move into SE-CC complex actively by means of sucrose-H^+ symporters. Sucrose- H^+ symporters are proton pumps associated with the plasma membranes of SE-CC complexes creating proton gradients and providing the energy needed to drive the transport of sucrose into the SE-CC complex (Taiz and Zeiger, 2006). The exact mechanism of apoplastic loading of sugars and carbohydrates is not well understood. Symplastic phloem loading includes the movement of sugars, carbohydrates, proteins, nucleic acids and other macromolecules from source photosynthetic cells (mesophyll or parenchyma) into the SE-CC complex via plasmodesmata. The movement of photosynthate from SEs to sink cells is called phloem unloading. Similar to phloem loading, unloading can occur via apoplastic and symplastic transport.

Vascular anatomy of *Nicotiana* and *Brassica*

This research will examine the movement of dyes and proteins in the vascular of two plant species. These plants are *Nicotiana benthamiana* and *Brassica oleracea*, which belong to the *Solanaceae* and *Brassicaceae* families, respectively. The section below will discuss the vascular anatomy of these plants, identify similar and unique components that determine the pathways for movement of dyes and proteins between organs and leaf veins.

The petiole has a single broad bundle that is U-shaped in the vascular arc (Fig. 1a, c). The bundle is in the center of the petiole cross section and is bicollateral, meaning that each bundle has external and internal phloem, and xylem vessels in the center (Fig. 1a and c)(Metcalfe and Chalk, 1979). Xylem and phloem chlorenchyma surround the vascular bundle in the petiole (Mekuria et al., 2008).

Compared to *Nicotiana benthamiana*, *B. oleracea* has more vascular bundles per petiole cross section (Fig. 1b). The petiole of *B. oleracea* is triangular in shape and has a single U-shaped layer of collateral vascular bundles. The phloem occurs on the abaxial side of the xylem (Fig. 1d). More than five bundles can occur per cross section and these vary in diameter, independent of position in the cross section (Fig. 1b). The larger bundles, represented in Fig. 1d, are fan-shaped while smaller bundles are circular. The *N. benthamiana* and *B. oleracea* petiole differ in the arrangement and number of xylem and phloem vessels and these could be factors affecting the rate and quality of mass flow into the leaf from the stem. The research present in this thesis examines the flow of dyes and proteins into sink petioles and leaves in each of these plant species.

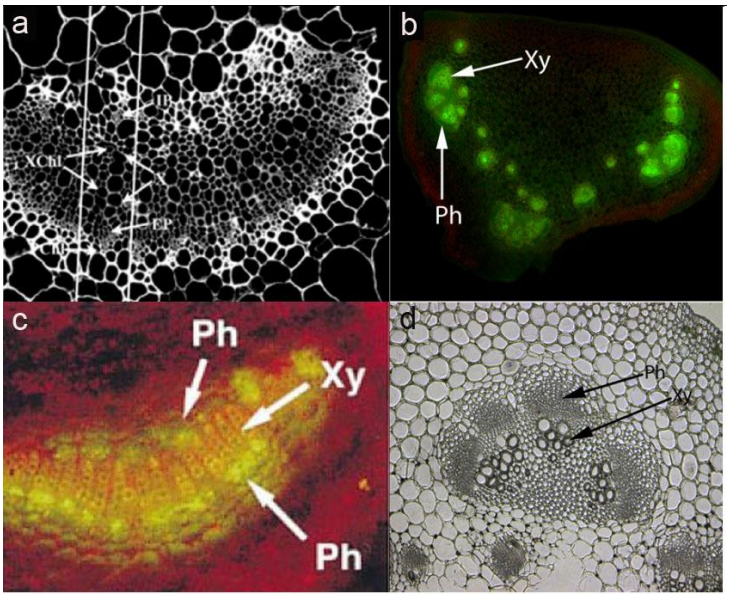

Figure 1. Vascular structure of *Nicotiana benthamiana* and *Brassica oleracea*.

(a) Cross section of tobacco petiole taken from Mekuria et al., (2008). Image shows detailed vascular anatomy, which is similar to the vascular arc of tobacco midvein drawn by Avery (1933). EP, external phloem; IP, internal phloem; X, xylem; PChl, phloem-associated chlorenchyma; XChl, xylem-associated chlorenchyma.

(b) Cross section of *B. oleracea* petiole taken using epifluorescence microscopy and 4x magnification. Carboxyfluroescein dye was loaded into the veins and highlights the phloem. Arrows point to phloem (Ph) and xylem (Xy).

(c) Cross section of *N.benthamiana* petiole (Imlau, Truernit, and Sauer, 1999). Image shows strong green GFP fluorescence in both regions of the phloem in AtSUC2 promoter–GFP tobacco plant. Ph, phloem; Xy, xylem.

(d) Cross section of *B.oleracea* vascular bundle located in the petiole and photographed using a 20 x objective (obtained from Dr. James Anstead, Dr. Gary Thompson's laboratory, Pennsylvania State University). Arrows point to phloem (Ph) and xylem (Xy).

Venation and vein classification

The veins contain an arrangement of vascular bundles and form characteristic branching patterns that are specific to each plant species (Esau, 1975). There are two general types of venation patterns in a leaf, netted and parallel. Netted venation is common among dicotyledonous plants, with smaller veins branch from larger veins. Major veins are typically identified as class I, II, and III. Minor veins are class IV and V. In contrast, parallel venation is a feature of monocotyledonous plants. Parallel veins are similar in size and are longitudinally arranged, approaching to the same point at the leaf apex, or branch from a similar origin near the petiole (Esau, 1975; Metcalfe and Chalk, 1979).

The venation patterns of *N. benthamiana* and *B. oleracea* are pinnate (Fig. 2). In leaves of *N. benthamiana* and *B. oleracea*, a prominent midrib divides the leaf blade into two parts, left and right. The midrib, class I vein, extends from the petiole to the top leaf apex, with smaller veins of several distinct vein size classes branching from larger veins (Fig. 2). Class II veins branch from class I. Class III veins are major veins that branch from class II veins. Class IV and V are minor veins that branch from class III and can be small in diameter. In Fig. 2, the vein classification system that was described for *Nicotiana tabacum* and *N. benthamiana* (Avery, 1933; Ding et al., 1988; Roberts et al., 1997) was applied to identify analogous vein classes in *B. oleracea* leaves.

N. benthamiana class II and III veins extend toward the leaf margin but bend away before they intersect with the margin. This is known as a camptodromous subtype of venation. For *B. oleracea* leaves class II and III veins intersect with the leaf margins, which is known as a craspedodromous subtype of venation. In *N. benthamiana*, but not

B. oleracea, the class III veins can intersect to create islands on the lamina that contain class IV and V veins in the interior (Fig. 2a, b).

The leaf veins of *B. oleracea* are light colored (Fig. 2b) making class I, II and III veins easily distinguishable. The class IV and V minor veins are not as obvious as the major veins. Perhaps because the leaves are thicker than *N. benthamiana*, the minor veins are less apparent.

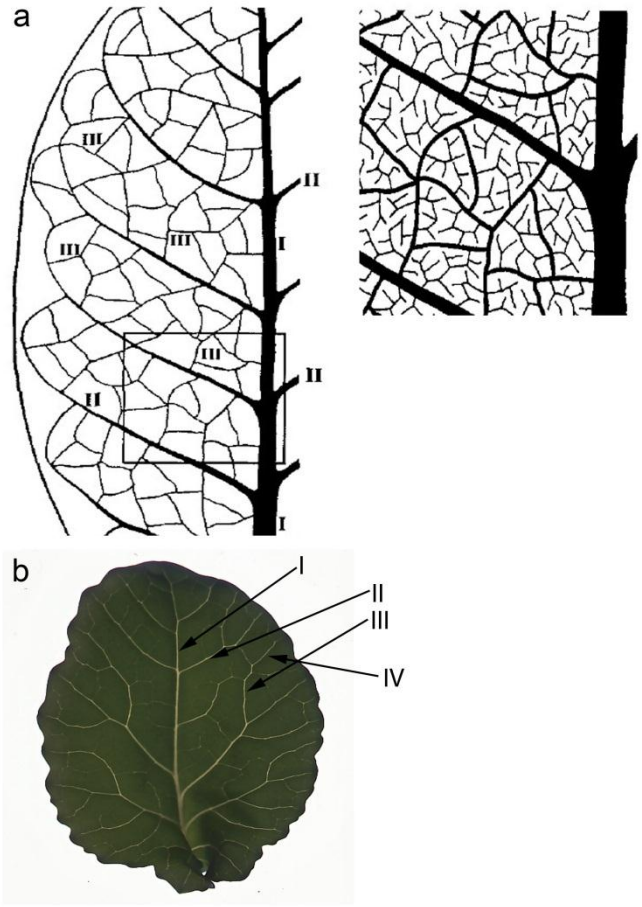

Figure 2. Comparison of vein patterns between leaves taken from *N. benthamiana* and *B. oleracea* plants.

(a) Venation of *N. benthamiana* leaf (Roberts *et al.*, 1997). Left picture shows class II veins branch out pinnately from class I vein in regular intervals and the right picture shows detail of minor veins' netted arrangement. (b) Venation of *B. oleracea* leaf. I, class I vein; II, class II vein; III, class III vein; IV, class IV vein; V, class V vein.

Loading veins and unloading veins

Sugars, proteins, and other macromolecules that are synthesized in the mesophyll of source leaves are transferred via plasmodesmata to the parenchyma or chlorenchyma cells next to the SE-CC complex. The process of phloem loading is the short-distance transfer of macromolecules from the CC directly into the SE for long distance transport to sink tissues. Macromolecules move by long-distance transport to different sinks (e.g. young developing leaves and flowers). Source leaves contain loading veins, also called minor leaf veins (class IV and V veins), which function to load proteins and sugars from the mesophyll and carry them to the major veins for trafficking into sink tissues. In sink tissues the major veins are known as unloading veins from which macromolecules exit into surrounding nonvascular tissues. There are also intermediate leaves that represent a transition between sink and source. In these leaves class I veins are bidirectional providing both import and export of macromolecules. Class II and class III veins may have phases of import and export of macromolecules. Class IV and V veins are typically importing macromolecules from the mesophyll in transitional leaves (Roberts *et al.*, 1997).

Virus movement may not conform to the traditional explanation for transport of solutes (dyes) and sugars. For example, *cowpea mosaic virus* (CPMV) can be loaded into both minor and major veins by using surgical isolation procedure method in cowpea leaves (Silva *et al.*, 2002). In regard to unloading of CPMV, only major veins are involved, especially class III veins (Silva *et al.*, 2002). However, green fluorescent protein (GFP) expressed in *Arabidopsis* source leaf companion cells can be unloaded symplastically. GFP unloading is mainly from class I, II and III veins, but not from

minor veins (Imlau, Truernit, and Sauer, 1999). Thus GFP appears to follow the pathway of phloem loading and unloading described by Roberts et al., (1997) for solutes. There is no evidence of endogenous proteins exiting minor veins and this may be due to the lack of tools to explore protein trafficking in leaf veins.

Our laboratory has reported transgenic plants containing GFP fused to the CC specific *Commelina yellow mosaic virus* (CoYMV) promoter. These plants were used to study GFP transport from the developing phloem in minor veins into neighboring tissues. Since the CoYMV promoter is turned on early in vascular development, GFP can be seen in immature phloem. Mekuria et al. (2008) reported that protein turnover in cells neighboring minor veins may be greater than surrounding major veins, giving the appearance of restricted flow in the minor veins. Changes in plasmodesmatal size exclusion limit (SEL) have been demonstrated through coinjection of phloem proteins with fluorescein isothiocyanate (FITC)-labeled dextrans into mesophyll cells of *Cucurbita maxima* (Balachandran *et al.*, 1997). This coinjection increased SEL of mesophyll plasmodesmata to 20 and 40 kD, but without phloem proteins, no SEL increase was found (Wolf, 1989).

Plant viruses achieve transportation in plants by adapting plasmodesmata. Some viruses (e.g. *Tobacco mosaic virus* [TMV]) moves through plasmodesmata modified by viral movement protein (MP) in a non-virion form (Carrington *et al.*, 1996). Other viruses, such as CPMV, use virus-induced tubules as a transportation intermedium to cross walls between neighboring cells (Van Lent, 1990; Van Lent, 1991). Many plant viruses, such as TMV, *Potato virus X* (PVX), *Cowpea mosaic virus* (CPMV), and *Potato virus Y* (PVY)

are able to exit the phloem of major leaf veins, but are detained in minor veins (Ding et al., 1988; Roberts et al., 1997; Silva et al., 2002).

Source-to-sink transport of proteins in stems

There are studies of CF dye and GFP source-to-sink transport in transitional leaves, but there are no reported studies of endogenous plant proteins in transitional leaves. However, there are studies of plant proteins moving with the flow of assimilate in the stems of grafted plants. For example, in *Cucurbita* the structural P proteins form filaments which function to plug the sieve plate in response to wounding (Golecki, Schulz, and Thompson, 1999). There are two major monomers of P proteins, PP1 and PP2, which are synthesized in CCs. PP1 monomers and PP2 dimers can move through the phloem, and in grafted plants, were observed to move across the graft union from root stock into the scion. These observations infer movement follows mass flow from a source to sink direction. PP1 monomer and PP2 dimers were detected in sink petioles. It is not known whether PP1 or PP2 can be translocated into leaf veins (Golecki, Schulz, and Thompson, 1999). Research has also shown that the transcription factor, Flowering Locus T (FT), which is required for flowering, is synthesized in CC in leaves and moves via the phloem into the apical meristem (Giakountis and Coupland, 2008). Transgenic tomato rootstocks expressing FT from the CaMV 35S promoter were grafted with *ft* mutant scions defective in FT production. These experiments showed that the FT protein is graft transmissible (Giakountis and Coupland, 2008). The FT protein was not reported in the petioles or sink leaves suggesting that either it is degraded in these locations or is

blocked from entering these tissues. These reports on P proteins and FT suggest that the phloem transport of certain proteins is regulated, somehow controlling their destination and selective export, and differs from simple small molecules.

Technologies currently used to track flow of proteins in plants via the phloem

GFP is a great tool for studying protein transport through the phloem because it is relatively resistant to chemical and physical treatments, such as heat, alkaline pH, detergents, or organic solvents (Bokman and Ward, 1981). Its crystal structure is a barrel-like shape cylinder, which is 42 Å x 24 Å (Ormö *et al.*, 1996). GFP is excited with blue light and can be visually monitored in the phloem through nondestructive techniques. In addition, GFP has been fused to *AtSUC2* and *CoYMV* promoters in transgenic *Arabidopsis* and tobacco where it is expressed only in phloem tissues. These plants have been used to monitor protein movement through the phloem, entering floral organs (petal, anther and ovules) and root tips (Imlau, Truernit, and Sauer, 1999).

Recombinant plant viral genomes expressing GFP have been used to monitor the paths of virus movement through the phloem into various organs (Mekuria *et al.*, 2008; Silva *et al.*, 2002). The combination of GFP, transgenic technology and recombinant viruses have contributed to study phloem loading and unloading, as well as, determining the requirements for long distance transport.

Some other fluorescence technologies also have been used in study of vascular transport. Texas Red dextran has been used to study xylem transport while carboxyfluorescein (CF) has been used to monitor phloem transport (Grignon, 1989;

Roberts et al., 1997). CF dye is a polar fluorescein molecule that can be loaded into the phloem in source petioles and follows the flow of photoassimilates into sink tissues. CF dye can be used to monitor phloem sap translocation in real time, in short- and long-term experiments (Grignon, 1989).

Root and scion grafting are used to track movement of macromolecules through the stem. The scion tissue of one plant is affixed to the rootstock and encouraged to fuse. This technique is widely used in agriculture and horticulture. After a few weeks, the vascular cambium tissues of the rootstock and scion fuse, forming a successful graft. The vascular connection between the two tissues allows mass flow to carry molecules throughout the plant. Grafting also provides another way to study protein mobility in phloem, for example, GFP produced in the CCs of transgenic rootstock can enter the SEs and then be translocated into the nontransgenic scion (Mekuria et al., 2008; Taiz and Zeiger, 2006). However, grafting imposes specific stresses on the vasculature, and requires a long time for phloem vessels to fuse and perform normally. The quality of the phloem in the graft region is not always identical to the intact plant.

Recently, magnetic resonance imaging (MRI) technology has been employed for monitoring of vascular transportation in plants (Gussoni *et al.*, 2001). Since plants are largely composed of water molecules which each contain two hydrogen nuclei or protons. When plants are put inside the powerful magnetic field of the scanner, the magnetic moments of these protons align with the direction of the field. A radio frequency electromagnetic field is then briefly turned on, causing the protons to alter their alignment relative to this second electromagnetic field. When this radio frequency field is turned off the protons return to the original magnetization alignment. These alignment changes

create a signal, which can be detected by the scanner. This technology can non-destructively and non-invasively measure vascular transport in intact plants. MRI technology is widely used for studying vascular transport in mammalian systems and has been employed in few plant biology studies to describe flow dynamics, as well as, anatomical structures (Scheenen et al., 2002; Scheenen et al., 2007; Windt et al., 2006). MRI has been used for studying the long distance water transport in cucumber plants under normal and environmental stress conditions. Heavy water and gadolinium have been loaded into the vasculature as MRI tracers to quantify the vascular transport velocities in *Pharbitis nil* (morning glory) (Gussoni *et al.*, 2001).

In recent years plant viruses have been employed as tools for material applications. Their rigid capsid structures make them excellent choices for molecular scaffolds. Virion surfaces of many icosahedral viruses can be easily chemically modified for the attachment of peptides, polysaccharides, nucleic acids, fluorescent or magnetic dyes, or other synthetic structures (Loo et al., 2007; Loo et al., 2008; Sapsford et al., 2006). Most icosahedral viruses self-assemble in solution with significantly more uniformity than can be achieved with synthetic structures. Plant viruses such as CPMV, *Cowpea chlorotic mottle virus* (CCMV), *Red clover necrotic mosaic virus* (RCNMV) and *Brome mosaic virus* (BMV) are examples of viruses that have been used for material and biomedical applications (Lewis et al., 2006; Loo et al., 2007; Loo et al., 2008; Manchester and Singh, 2006; Sapsford et al., 2006).

Research Objectives

Generally, the components in phloem sap are sugars, amino acids, photoassimilates, proteins, nucleic acids and plant viruses (Carrington et al., 1996; Carrington and Whitham, 1998; Hall and Baker, 1972; Lucas and Wolf, 1999; Nelson and Dengler, 1997). This project investigates whether exogenous proteins and virus protein transport depends upon sap flow within the stem and petiole phloem, reveals if plants differentiate exogenous proteins with respect to transport and post phloem sorting. Protein unloading in leaf veins was also tracked. The results of this research will be used as the foundation information for lab future study of engineered virus nanoparticles delivery to target tissues. This research compares the vascular transport properties of two plant species. The specific goals are:

1. To characterize long distance transport of dyes in *N. benthamiana* and *B. oleracea* by fluorescence technology
2. To characterize long distance transport of fluorescence conjugated proteins by fluorescence and MRI imaging technology.
3. To investigate biodistribution of virus protein in intact plants.

CHAPTER II

EXPERIMENTAL MATERIALS AND METHODS

Plant Materials

Seeds of *Nicotiana benthamiana* and *Brassica oleracea* were sown in Metro-Mix and grown in a growth room with 16 h light at 25 ℃. The age of plant was determined by the number of fully expanded leaves, which were four to five for *N. benthamiana* and four for *B. oleracea* in all the experiments. Plants analyzed under hydroponic conditions (in growth pouches) were first grown in soil to ensure vigor. Then plants were removed from soil, the roots will be quickly rinsed in water and plants were transplanted to growth pouches (Fig. 3). After transplanting, growth pouches were placed in a growth room for 24 h prior to the experiment to ensure plants were adapted to the liquid growing environment to ensure maximal water conductivity in all tissue for experiments.

Figure 3. Example of growth pouches (hydroponic bags) for growing and maintaining plants. Plants growing in soil produce stronger stems, larger leaves and are taller than plants grown in the hydroponic bags during the experiment preparation. Therefore, for accurate physiological comparisons of phloem transport, all plants were grown in soil first and then a subset were moved into the bags prior to experimentation.

Fluorescence Imaging

To measure mass flow through the stems and into sink petioles and identify loading/unloading veins, fluorescent compounds were introduced into the roots or petiole of first source leaf (Leaf 1). The fluorescent compounds used in experiments were 60 μg ml^{-1} 6 (5)-carboxyfluorescein (CF; Sigma, St. Louis, MO) according to standardized protocols (Roberts et al., 1997; Yang et al., 2000). Histone H1-Alexa Fluor488 from calf thymus (34 kDa; Invitrogen, Carlsbad, CA), bovine serum albumin-Alexa Fluor488 (66 kDa; Invitrogen, Carlsbad, CA) and *Hepatitis C virus* core antigen-Fluorescein (136kDa; Sigma, St. Louis, MO) were adjusted to 0.3 mg ml^{-1}, 0.3 mg ml^{-1} and 0.09 mg ml^{-1}, respectively to achieve comparable fluorescence intensity to that of 60 μg ml^{-1} CF dye (Table 1).

The application of CF dye and fluorescent proteins in L1 petiole and root were conducted separately in soil grown or pouch-grown plant (Fig. 3). Soil grown is the normal condition for plant growth, and was used to compare the role of sap flow in protein delivery in hydroponic media. The pouch hydroponic medium would provide greater water content to root systems and result to greater flow in the vasculature than soil-based growth media (Li *et al.*, 2002). Hydroponic growth medium was also preferred for MRI analysis since the water in the soil affects the results and contaminants in the MRI machine is forbidden.

Table 1. The concentration and absorbance value of fluorescent dye and proteins

Fluorescence dye or proteins	MW	λ488
60 μg ml^{-1} Carboxyfluorescein dye	460 Da	1.847
0.3 mg ml^{-1} **Histone** H1 from calf thymus - Alexa Fluor488	34 kDa	1.810
0.3 mg ml^{-1} **Bovine serum albumin** - Alexa Fluor488	66 kDa	1.882
0.09 mg ml^{-1} **Hepatitis C virus core antigen** - Fluorescein	136 kDa	1.834

Two dye/protein delivery methods were used in the soil grown and pouch-grown experimental plant, respectively. In petiole application experiments, the L1 leaf was detached at the connection point between petiole and leaf lamina. The cut surface of the petiole was inserted into a 600 µl eppendorf tube filled with 300µl CF dye, Alexa-Histone or Alexa-BSA and secured to the petiole using parafilm. In root application experiments, the cut surface of main root was inserted into the 600µl eppendorf tube filled with 300µl CF dye, Alexa-Histone or Alexa-BSA and secured to the root using parafilm.

In preliminary experiments, the progression of CF dye or proteins from the petiole to the upper leaves was monitored using a hand held UV Blue-Ray lamp (UVP, LLC, Upland, CA). This assisted to determine the time it took for dye or proteins to reach young leaves. Moreover, time course experiments were designed to identify the key intervals for studying transport velocity and vascular unloading in leaves. To quantify CF dye or proteins in the petiole vasculature, cross sections of the source and sink petioles were imaged using a Nikon E600 epifluorescence microscope (Nikon Corp., Tokyo, Japan) equipped with a 470-490 nm excitation filter, a DM505 dichroic mirror and a BA520 barrier filter, and a built-in Magnafire camera. Then images were analyzed using Image J software. The vascular areas in the petiole cross sections were circled in Image J and the fluorescence intensities (green channel) were quantified by the software and recorded with Excel spread sheets. The volume dimensions of the fluorescent regions of the vasculature were recorded and reported as FU mm^{-3}. These values were plotted using Excel spread sheets. The FU mm^{-3} and time of transport was determined based on changes of volume between the origin and destination petioles in each plant species. The

velocity of transport of each petiole, the effects of soil versus hydroponics on transport, and the effects of petiole application versus root application on transport were compared.

Intercellular Wash Fluids (IWF) Extraction and Protein Extraction from Leaf

Leaves from control, Alexa-BSA or -Histone treated plants were excised and carefully washed with deionized water and blotted dry. Leaves were infiltrated with a needleless syringe containing 1 ml 180 mM 2-[N-morpholino]ethane-sulphonic acid (MES) and then blotted dry again. Leaves were transferred to centrifuge tubes and centrifuged immediately at 230 g, for 4 min at 4 ℃. The liquid (intercellular wash fluid) in the centrifuge tube was collected for SDS-PAGE and immunoblot analysis. Crude extracts of the remaining leaf tissue was ground with grinding buffer (100 mM Tris-HCl, pH7.5, 10 mM KCl, 5 mM $MgCl_2$, 400 mM sucrose, 10% glycerol and 10 mM β-mercaptoethanol) at a ratio of 0.1 g leaf tissue per 100 μl buffer and the debris were centrifuged out. The intercellular wash fluid and leaf extracts were diluted with equal vol of tris-glycine SDS gel loading buffer (Invitrogen). Samples were boiled for 5 min in water-bath, then the tubes were transferred to ice for 3 min, then centrifuged at 13,200 rpm for 5 min before loading to SDS-PAGE gel.

SDS-PAGE, Immunoblot Analysis and Silver Stain

IWF and leaf tissue protein were separated by 15% (for Histone experiment) or 8% (for BSA experiment) SDS-PAGE. After electrophoresis, the duplicate gels were either silver stained or transferred to a PVDF membrane (GE healthcare, Piscataway, NJ) by electroblotting with a TransBlot apparatus (Bio-Rad, Hercules, CA) according to manufacturer instructions. Blots were incubated with anti - histone antibody (1:200 [v/v], polyclonal; Santa Cruz Biotechnology Inc., Santa Cruz, CA.) or BSA antibody (1:3000 [v/v], polyclonal; Invitrogen, Carlsbad, CA) for 1h. The secondary antibody, ECL anti-rabbit IgG (GE healthcare, Piscataway, NJ) was diluted to a ratio of 1:20000 for histone detection or 1:50000 for BSA detection and incubated for 1 h. Chemiluminescent detection was used to reveal the Histone or BSA band. The detection agent (GE healthcare, Piscataway, NJ) was removed from storage at 4℃ and equilibrated to room temperature before opening. Then the detection solutions were mixed in a ratio of 40:1 (1 ml solution A + 25 µl solution B per membrane). The excess wash buffer was drained from membranes and protein side was placed up on a sheet of SaranWarp. The mixed detection reagent was pipette on to the membrane. The membrane was covered with another sheet of SaranWarp and excess detection agent was drained off by filter paper. The membrane was incubated in x-ray film cassette for 5 min at room temperature. In dark room, a sheet of autoradiography film (Fisher, Hanover Park, IL) was placed on top of membrane in x-ray film cassette exposed the film vary from 1 min to 1 h.

Silver staining was carried out as described previously (Maniatis, Fritsch, and Sambrook, 1982). Briefly, SDS-PAGE gels were incubated in 45 ml fixative solution (30% ethanol, 10% acetic acid) for 12h at room temperature with gentle shaking. After discarding the fixative, gels were washed twice with 5 gel vol of 30% ethanol for 30 min.

After discarding the ethanol, the gels were washed 5 times with 10 gel vol of ddH_2O for 10 min each. For staining, gels were immersed in 5 gel vol of 0.1% $AgNO_3$ (freshly diluted from 20% $AgNO_3$) for 30 min. Then the gels were washed under a stream of ddH_2O for 20 sec on each side, and then immerse in 5 gel vol of freshly made developer (2.5% sodium carbonate, 0.02% formaldehyde) for several min. After bands appeared on the gel, the reaction was quenched by washing the gel first with 1% acetic acid for a few min, and then several times with ddH_2O (10 min per wash).

Magnetic Resonance Imaging Technology

Tracer solutions of gadolinium-diethylenetriamine pentaacetic acid (Gd-DTPA, 938 Da, Magnevist) and biotinyl-bovine serum albumin-gadolinium-diethylenetriamine pentaacetic acid (Gd-BSA, 90 kDa) were applied to plant roots to and mass flow through the stems were measured by MRI. The tracers would follow bulk flow through the plant vasculature to upper leaves. These experiments provided a quantitative measure of protein transport in the stem. A MRI spin labeling sequence was used to characterize flow velocities in the stems. Apparatus was designed to hold the plants inside the MRI that would be used to measure vascular flow. Gadolinium-based contrast agents are used to improve the visibility of internal structures by MRI (Gussoni *et al.*, 2001; Osuga *et al.*, 1998). The small molecule Gd-DTPA should permit measure of phloem conductance and Gd-BSA, relatively a large protein, should permit determining protein transport velocity.

N. benthamiana plants (four fully expanded leaves) were removed from soil, the roots were quickly rinsed in water and immersed in a cup of water. Each plant, with its

roots placed into the cup, was fixed onto a narrow board that fits inside the MRI machine (Fig. 4a; Bruker Biospec 7.0 Tesla / 30 cm horizontal-bore magnet small animal imaging system (Bruker Biospin, Ettlingen, Germany). Then a leaf was covered with a filter paper to flatten it.

For all plants, Gd-DTPA or Gd-BSA was applied to the plant roots. One piece of tubing (diameter: 0.1 cm) was inserted into the water-filled cup containing the plant roots (Fig. 4c). A syringe was used to apply Gd-based molecule to the tubing. A larger second tubing (diameter: 0.5 cm), interrupted with a stop cock valve joint was also inserted into the water filled cup or conical tube. A 1 ml pipette tip is attached to one end and a bulb is used to push air into the cup. When the stop cock was open the air enters into the water and this mixes the water and Gd-DTPA or Gd-BSA into final concentration of 4.7 mg ml^{-1} and 1 mg ml^{-1} respectively (Fig. 4c). The reason for this set up is to stir the tracers into solution while the plant is in the MRI inner chamber.

The plant containing apparatus was placed into the MRI inner chamber (Fig. 4b). Then the machine was standardized by the MRI technician at OMRF. Gd-DTPA or Gd-BSA was applied to the roots using the apparatus, then stopcock valve on the second tube was opened. Air was pushed six times into the second tubing and the dye and water are mixed. Then the MRI scanning software was used to detect and measure flow rates in plant stems. Morphological details of vein in leaves were also recorded.

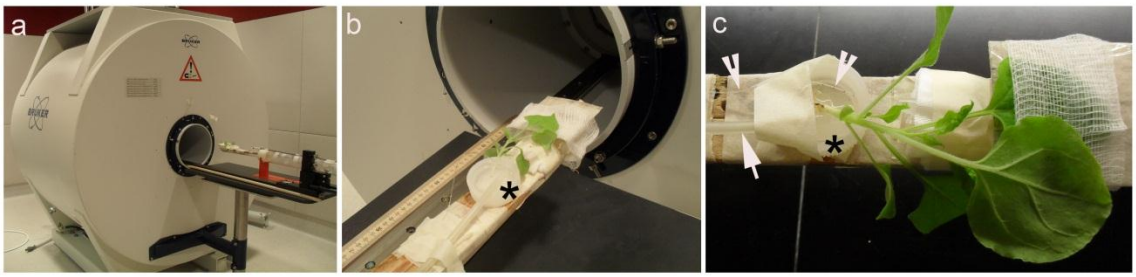

Figure 4. MRI set up for the *N. benthamiana* plants

(a) Bruker Biospec 7.0 Tesla / 30 cm horizontal-bore magnet small animal imaging system (Bruker Biospin, Ettlingen, Germany).

(b) The root of the *N. benthamiana* plant, placed into a cup, which is fixed on a narrow board. The board has the appropriate size for the inner space of MRI machine.

(c) MRI apparatus for *N. benthamiana* plant. * indentifies the cup containing water before injection of Gd-DTPA or Gd-BSA. Arrowheads, tubing (diameter: 0.1 cm) used to apply Gd-DTPA or Gd-BSA, connected to a syringe; Arrow, tubing (diameter: 0.5 cm) used to inject air in to cup to mix water and Gd-DTPA or Gd-BSA connected to a stop cock valve joint (not shown). MRI were carried out using FLASH sequence with echo time = 7ms, repetition time = 300ms, matrix 384×256, field of view = 80mm×54mm. For leaf vein experiments, MRI were carried out using FLASH sequence with echo time (TE) = 6ms, repetition time (TR) = 376ms, matrix 256×256, field of view = 80mm×80mm.

CHAPTER III

RESULTS AND FINDINGS

Measuring fluorescence intensity in petiole cross sections as an indication of fluorescent protein transfer from the loading site into upper leaves

Carboxyfluorescein (CF) dye is a commonly used indicator of long distance phloem transport. A typical assay involves cutting the petiole of the leaf closest to the soil surface (L1) and attaching a vial of CF dye solution. L1 is the most mature leaf and is considered to be a source of photoassimilates that are transferred long distance through the phloem to sink leaves, which are less mature and unable to produce adequate photoassimilates needed for leaf expansion. In *N. benthamiana* plants, CF dye that is applied to the L1 petiole enters the phloem and unload in sink leaves, following the same route as photoassimilates (Roberts et al., 1997). On occasions CF dye can also enter the xylem (Roberts et al., 1997).

The above delivery method was employed for studying CF dye transport in the phloem and to deliver fluorescent proteins into the phloem of *N. benthamiana* plants. Commercially available Alexafluor488-BSA and Alexafluor488-Histone H1 (0.3 mg ml^{-}

^{1}) (here called Alexa-BSA and Alexa–Histone) were loaded into the L1 petiole as described (Roberts et al., 1997), or were delivered to plant roots. Transport of CF and fluorescent proteins to distal tissues was monitored in upper leaf petioles. CF dye (60 μg ml^{-1}) was used as a positive control. Importantly the solutions were prepared such that the concentrations applied to the plant produced similar absorbance values. Leaves were numbered L1 to L5 in their order of emergence above the soil, such that L1 was the mature source leaf that lay closest to the soil surface and L5 was the youngest sink leaf to emerge. Leaf petioles were detached, and 0.5 mm sections were placed on slides and examined microscopically at 10, 30, 60, and 90 min post-delivery of proteins to *N. benthamiana* plants. Fluorescent images were recorded and Image J software was employed to measure the fluorescence intensity levels in the central vascular bundle.

Fig. 5 shows a comparison of representative L4 petiole cross sections. The intensity of fluorescence due to CF dye, Alexa-BSA, or Alexa-Histone were visually comparable at 10 min but the amount of fluorescence varied significantly among the applications to L1 petioles (Fig. 5a) between 30 and 90 min suggesting that phyllotaxy or sap flow in the phloem were not the sole factors governing the amount of fluorescence seen in comparable tissues. For CF dye the fluorescence intensities in the central vascular bundle of L4 petioles at 30 and 60 min was comparable. There are two lateral veins along the adaxial side of the petiole that also showed CF dye fluorescence (Guo et al., 2010; Maksymowych, Orkwiszewski, and Maksymowych, 1983). For Alexa-BSA the fluorescence in the central vascular bundle was lower than CF and there was no obvious fluorescence in the lateral veins. One explanation is that diffusion of Alexa-BSA (66 kDa) in the phloem might not be comparable to CF dye because it is a significantly

larger molecule. This is contrasted by the 34 kDa Alexa-Histone which is smaller than BSA and resembles plant endogenous histones. Fluorescence in the L4 petiole cross sections containing Alexa-Histone was greater than BSA at 30 min, with some evidence of fluorescence in one lateral adaxial vein (Fig. 5a), but fluorescence declined until 60 min. To better compare our observations, fluorescence in L4 petiole cross sections was quantified and determined by the average (n=4) fluorescence units (FU) per mm^3. These data were presented graphically over time and better depict our qualitative observations. Namely, CF dye and Alexa-Histone uptake initially showed peak fluorescence in L4 petioles at 30 min. Alexa-Histone levels are approximately 50% of CF dye at 30 min. While CF-dye reached a plateau, Alexa-Histone declined. A second rise in fluorescence accumulation in L4 petioles is noted at 90 min. Thus the pattern of uptake is not linear over time. It is possible some CF dye leaks into the symplast and this causes a temporary plateau as the tissue reaches homeostasis before the second increase. It was noticed that faint fluorescence occurred in some mesophyll cells, which support this assertion. A second explanation is that the sap pressure inside the phloem is not constant and so there are periods of sap movement followed by static periods. With respect to Alexa-Histone the decline in fluorescence is likely due to protein degradation and greater movement of fluorescence into surrounding nonvascular cells (see below). The second increase in fluorescence transfer to L4 petioles that occurs between 60 and 90 min mirrors the increase seen in CF dye treated plants.

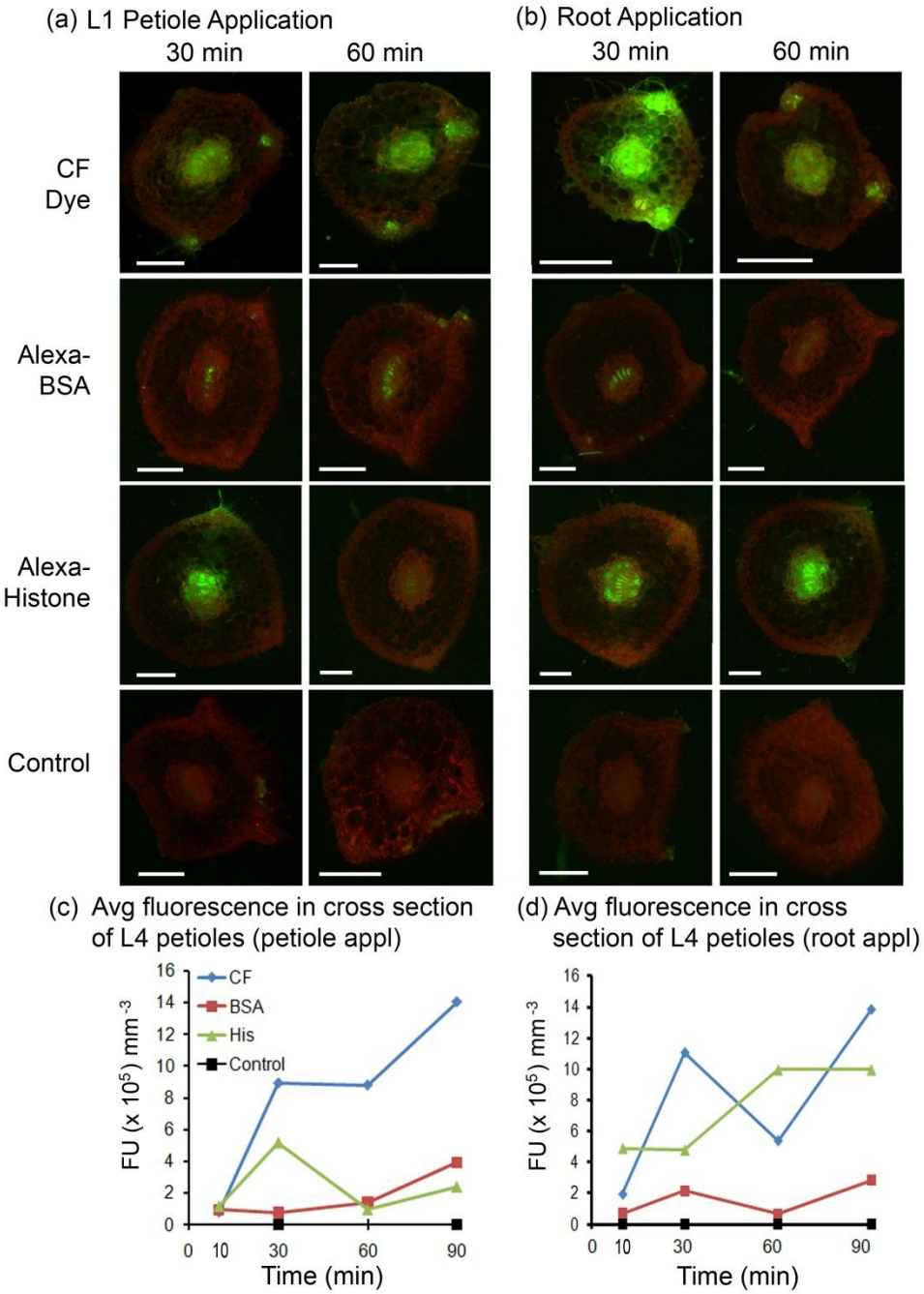

Figure 5. Images of L4 petiole cross sections of *N. benthamiana* and average fluorescence intensity of L4 petiole cross sections. (n=4) (a) following L1 petiole (b) following root application at 30 and 60 min. Plants were treated with CF dye, Alexa Fluor 488 BSA and Alexa Fluor 488 Histone H1. Bar = 500 μm. Two lateral veins along

the adaxial side of the petiole also showed CF dye fluorescence (Agrios, 1969; Guo et al., 2010; Maksymowych, Orkwiszewski, and Maksymowych, 1983). (c) and (d) graphically depict the average fluorescence values (n=4) in the central vascular bundles of L4 petiole cross sections. CF dye reached a maximum at 30 min and declined until 60 min. Uptake of Alexa-BSA is low when delivered to the roots. However, Alexa-Histone uptake is greater in the first 10 min following delivery to the roots than the L1 petiole. The amount of Alexa-Histone that transfers to L4 petioles reaches saturation and a plateau at 60 min.

In contrast, Alexa-BSA shows a linear increase in fluorescence over 90 min, although the amount of fluorescence is significantly lower than CF dye or Alexa-Histone. The intensity of Alexa-BSA in the central vascular bundle is approximately 14% of CF dye. The performance of CF dye, Alexa-BSA, and Alexa-Histone are not identical suggesting that the physical properties of the fluorescent dye and proteins (tertiary structure, charge, molecular mass) have a greater influence than phyllotaxy over their transport.

Following root delivery, the fluorescence intensities of CF dye, Alexa-BSA, and Alexa-Histone in the vascular bundles of L4 petioles over time differed from that of fluorescence intensities following petiole delivery. Fluorescence microscope inspection of cross sections of L4 petiole showed CF dye intensely staining the vascular bundle and surrounding tissues within 30 min of delivery. It was possible that the dye was in the apoplast as well as the symplast. CF dye reached a maximum at 30 min, declined until 60 min and then rose until 90 min (Fig. 5b). One explanation is that the dye is degraded in the apoplast between 30 and 60 min and then there is a second increase in uptake. The other explanation could be that between 30 to 60 min post-delivery of CF dye, the sap flow transfer rate in leaf 4 petiole from stem to leaf increased suddenly, but the import of CF dye was not as fast as CF output from petiole to leaf, which made the amount of CF dye in petiole decreased significantly and reduced the fluorescence of L4 petiole cross section. The biphasic kinetics could also be due to there are different types of transport systems for CF dye.

Root uptake of Alexa-BSA was similarly low as when delivered through the L1 petioles. However, Alexa-Histone uptake was greater in the first 10 min following

delivery to the roots than through the L1 petiole. Images in Fig. 5b show fluorescence due to Alexa-Histone in the xylem as well as phloem. The amount of Alexa-Histone that transferred to L4 petioles reached a plateau at 60 min.

These data revealed protein specific patterns of transfer into sink leaves from the L1 source leaf and roots. The larger BSA moved slowly to the L4 petiole, while small histones transported more rapidly, especially following root delivery (Fig. 5a, b).

Protein accumulation in symplast and apoplast

Confocal microscopy was employed to visually assess the presence of fluorescence in vasculature and surrounding tissues. Following root application, CF dye was seen mainly in the sieve element-companion cell (SE-CC) complex and in phloem parenchyma cells (Fig. 6a). Thus evidence of dye spreading beyond the SE-CC complex supported the notion that a decline in fluorescence between 30 and 60 min reported in Fig. 5b may be due partly to dye leaking into surrounding tissues. On the other hand, following petiole application, CF dye was mainly in the SE-CC complex, with much less fluorescence in surrounding parenchyma (Fig. 6b). This also supported the notion of a plateau between 30 and 60 min reported in Fig. 5a, where fluorescence did not appear to leak out of the phloem into surrounding tissues.

As in Fig. 5, 90 μg of Alexa-BSA were delivered in a solution to the roots or L1 petioles and in both cases fluorescence did not appear to significantly enter the phloem (Fig. 6a, b). Fluorescence was mainly observed in the tracheary elements of the xylem. The low levels of fluorescence depicted graphically in Fig. 5 suggests that our

measurements reflect low levels of phloem trafficking. Given the lack of fluorescence in the phloem, L3 and L4 leaves were infiltrated with MES buffer and the intercellular wash fluid was pooled and analyzed by SDS-PAGE and silver staining to determine if proteins were present in the apoplast where they might be transported long distance (Fig. 6c). The leaf extracts of the remaining L3 and L4 tissues was analyzed by SDS-PAGE and silver staining to confirm intracellular protein accumulation (i.e.symplast). The proteins were quite dilute in the apoplast wash and only 11-17 μg were loaded to the gel (lanes A), while leaf extracts containing 40 μg total protein were loaded (lanes S). The leaf extracts and apoplast wash appeared to contain less than 1 μg of Alexa-BSA. Surprisingly accumulation of Alexa-BSA in intercellular spaces was greater following L1 petiole delivery of proteins than the root delivery. Immunoblot analysis using BSA sera confirmed Alexa-BSA associated with both intercellular wash fluids and cellular extracts (Fig. 6d). Both the silver stained gel and immunoblot indicated that less Alexa-BSA reaches the L3 and L4 petiole via a symplastic or apoplastic route following root delivery than petiole delivery. One explanation is that the proteins have to move a longer distance to reach the L3 and L4 leaves following root delivery than L1 petiole delivery.

90 μg of Alexa-Histone was delivered in to the roots or L1 petioles following same procedure as Alexa-BSA delivery (Fig. 5). Alexa-Histone was distributed throughout the phloem and xylem including the parenchyma. There did not appear to be a preference for the SE-CC complex or tracheary elements as seen for CF dye or Alexa-BSA (Fig. 5 and 6a, b). Fluorescence did not appear in intercellular spaces suggesting that Alexa-Histone moved long distance via the symplast. As for BSA, the lack of phloem tropism led us to determine if proteins accumulate in the apoplast or symplast.

Intercellular wash fluids and cell extracts pooled from L3 and L4 leaves were analyzed by SDS-PAGE and silver staining (Fig. 6c). Thirty to forty μg total protein were loaded to the gel and silver stained gels showed Alexa-Histone mainly in tissue extracts and not in the intercellular wash fluids, regardless of L1 petiole or root delivery. The Alexa-Histone migrated to a position in the gel that is slightly higher than the 34 kDa molecular weight marker probably because of the Alexa fluor conjugate affecting its migration through the gel. Immunoblot analysis also confirmed Alexa-Histone accumulated in cellular extracts (Fig. 6d). There was a second band in the immunoblot that corresponds to plant endogenous histones that cross-react with the same antisera. These data suggest that the decline in fluorescence seen in Fig. 5 might result from protein movement into surrounding tissues.

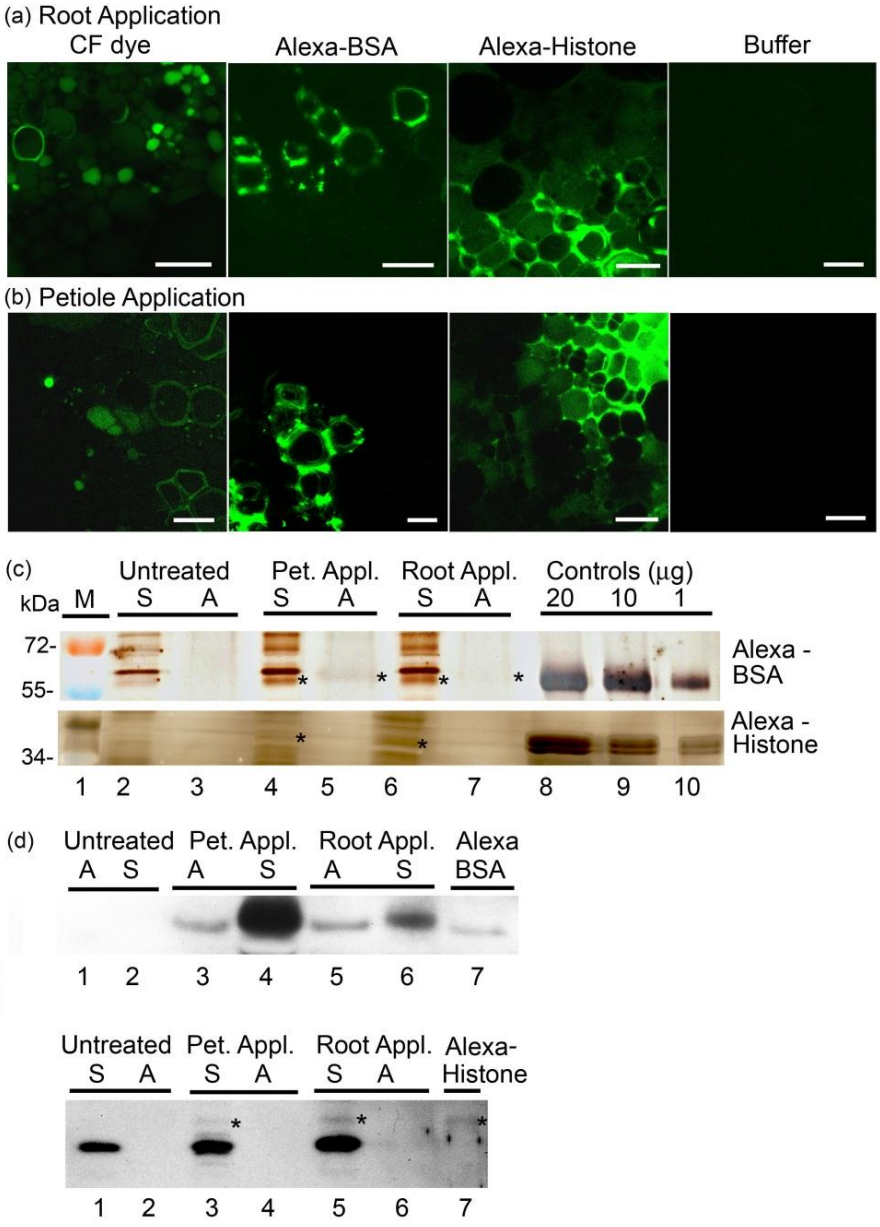

Figure 6. Analysis of symplastic and apoplastic accumulation of Alexa- BSA and Alexa-Histone H1 in *N. benthamiana* leaf.

(a, b) Confocal microscopic images of CF dye, Alexa-BSA and Alexa-Histone H1 in *N. benthamiana* petiole cross sections following root application (a) or petiole (b) application. Bar = 30µm. CF dye fills the phloem and is barely visible in xylem or

parenchyma cells. Alexa-BSA was mainly in the tracheary elements of the xylem. Alexa-Histone spreads beyond the phloem into parenchyma cells. Control samples were treated with buffer and show no fluorescence.

(c) Silver stained SDS-PAGE gel show accumulation of Alexa-BSA and -Histone at 90 min. Apoplastic wash fluids (A, lanes 3, 5, 7) and symplastic cell extracts (S, lanes 2, 4, 6) were pooled from L3 and L4 leaves. For the Alexa BSA gel, asterisks in each lane mark bands consisted with MW of Alexa-BSA in both the symplastic (S) and apoplastic (A) extracts. Alexa-BSA was directly loaded to gel and produces a band around 66 kDa. For Alexa-Histone, asterisks in lanes show Alexa-Histone in the symplast but not apoplast wash fluid. Alexa Histone control band is around 34 kD. Loading amounts (μg) for Alexa-BSA and -Histone are indicated above the lanes.

(d) Immunoblots og PAGE gels in (c), probed with polyclonal antisera detecting BSA and Histone. Pet. Appl, petiole application; Root Appl, root application; M, marker; Asterix indicates larger Alexa-Histone band. Endogenous histone H1 of *N. benthamiana* was also detected by antisera.

To summarize, three different size fluorescent molecules were employed to study transfer from application sites in the roots and L1 petioles to the L4 leaves: CF dye (460 Da), Alexa-Histone (34 kDa), and Alexa-BSA (66 kDa). These data indicate that the increasing size of the molecule reduces its ability to be transferred to distal leaves. Dye and proteins of smaller sizes moved better in the phloem than larger proteins, such as the 66 kDa Alexa-BSA. These data suggest that there might be a size limit for transfer via the phloem. The best explanation is that the sieve plate pore provides a physical restriction that might limit transfer of molecules distally. Regardless of root or petiole application, Alexa-BSA (but not –Histone) occurred in apoplastic wash fluids.

Protein transfer to upper leaf petioles of soil grown *N. benthamiana* plants

According to Roberts et al., (1997) transport of CF dye from an importing leaf is governed by phyllotaxy whereby carbon-based molecules transferred via the phloem reaches the closets leaves sooner than distal leaves. However, it is not known if protein transport involves targeting to specific locations or is also governed by phyllotaxy. This experiment monitored the transport of CF dye, Alexa-BSA and Alexa-Histone at 10, 30, 60, and 90 min post-delivery of by examining cross sections of L1-L5 petioles. Control plants were treated with buffer only.

The first observation following root application is that regardless of the CF dye or proteins applied, fluorescence reached all leaves simultaneously. The second observation is that transport is biphasic (Fig. 7a). There is an initial uptake phase followed by a plateau or decline in fluorescence, and then a second phase of uptake. With respect to CF

dye and Alexa-BSA there was an initial peak accumulation at 30 min followed by a slight decline. The second increase in fluorescence intensity occurs between 60 and 90 min and the fluorescence intensity slightly exceeds the maximum recorded at 30 min. The transfer of Alexa-Histone is also biphasic but occur earlier (Fig. 7a). The first uptake phase occurs within 10 min and is followed by a plateau, the rate of first phasic is 0.0404×10^5 FU s^{-1}. Between 30 and 60 min Alexa-Histone uptake reached a maximum that was comparable to the saturating levels reported for CF dye at 30 min. This Histone second uptake phase has a rate around 0.0033×10^5 FU s^{-1}. The first phase rate of root application Alexa-Histone is large than both CF dye (0.0071×10^5 FU s^{-1}) and Alexa-BSA (0.001×10^5 FU s^{-1}). The second phase rate of Alexa-Histone is still larger than Alexa-BSA (0.0011×10^5 FU s^{-1}) but similar with CF dye (0.0031×10^5 FU s^{-1}). The different rates of uptake suggest that there is an additional mechanism that speeds or slows uptake. It does not appear that increasing size of the proteins relative to dyes is the defining feature for initial transport, because Histone is larger than CF dye and its initial uptake by the petioles vascular is more rapid. Apoplastic transport cannot be considered as a positive factor for movement in the case of histone. Perhaps the ability of histone to spread further into surrounding tissues increases the pressure gradient within the sieve tube and increasing its uptake. In the vascular bundle where Alexa-Histone moving to SE-CC complex has a relatively a negative solute potential and causes a steep drop in the water potential. In response to the water potential gradient, water enters SE-CC complex and causes the turgor pressure. This pressure gives a chance for Histone to spread into surrounding tissue by following symplast pathway. The output of Histone from SE-CC

complex leads to a low histone concentration in the SE-CC complex generate a higher solute potential which helps to bring more histone to upper leaves from input site.

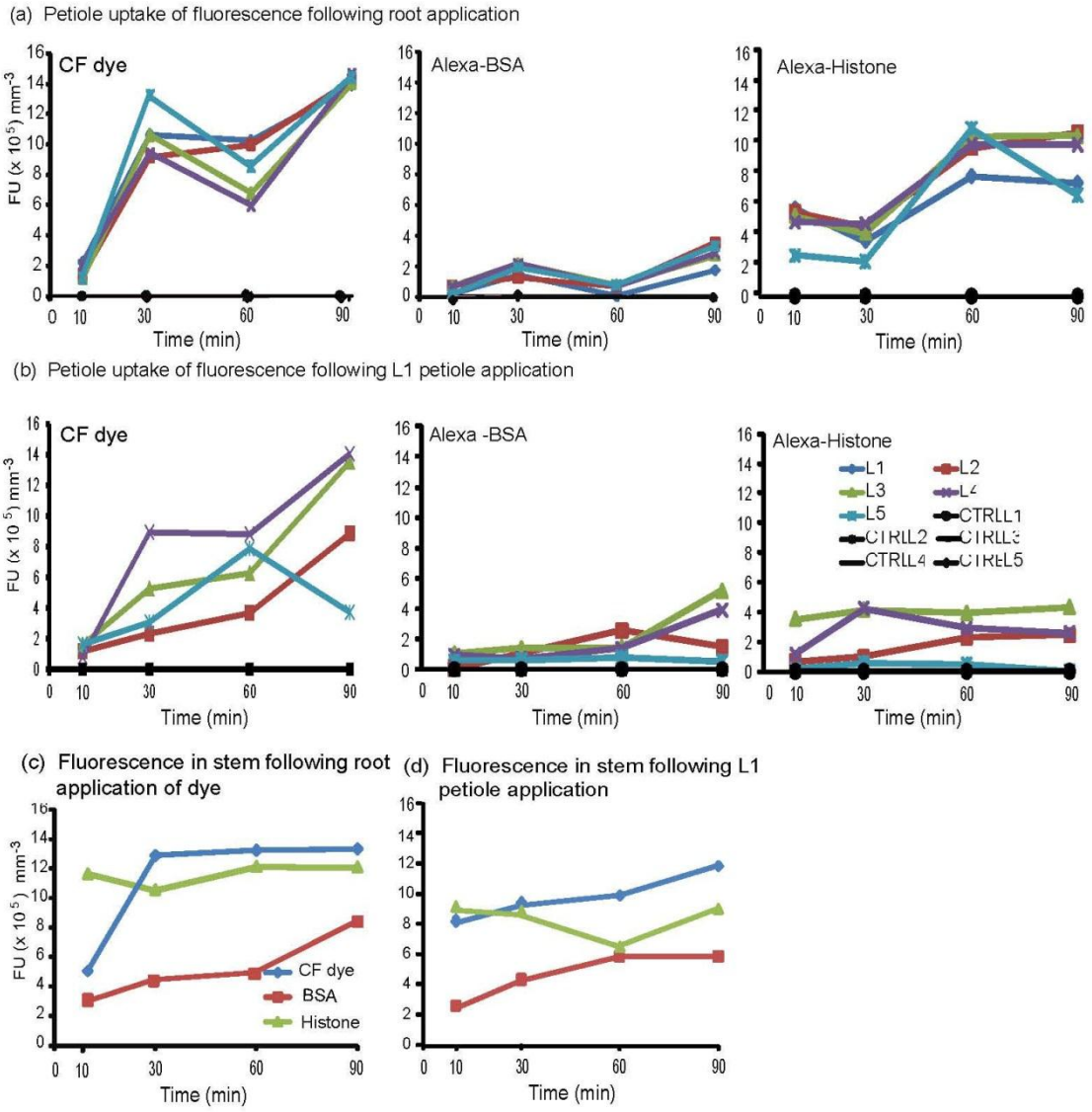

Figure 7. Fluorescence intensity of petiole and stem cross sections of soil grown *N. benthamiana* plants. Graphs depict the average fluorescence values in the central vascular bundles of (n=4) petiole (a, b) or stem (under L1 petiole) (c, d) cross sections, L1 values were not determined following L1 petiole application. The central vascular bundles were selected as regions of interest (ROIs) using Image J software and fluorescence values were recorded. Graphs depict the average values. The data were collected at 10, 30, 60 and 90 min after application of CF dye, Alexa-BSA or -Histone.

The decline or fluctuation in vascular accumulation of BSA was not observed as for histone. One possible explanation is that the plant might have an endogenous mechanism to regulate or degrade histones and the commercial product is recognized by the same pathway. BSA is not an endogenous protein in plants and may not be recognized by a targeted system. The comparison of histone and BSA therefore suggests that there might be protein specific rates of transfer and distribution, and possibly degradation during transfer to the various petioles.

Following petiole application, fluorescence intensities reach the first peaks on the same orthostichy as the L1 source leaf (Joy, 1964; Roberts et al., 1997). More CF dye and proteins were delivered into the leaves directly above the leaf 1 comparing to the fluorescence units of the leaves on the opposite side of leaf 1. CF dye applied to the L1 petiole produces the highest intensity at 30 min in L3 and L4 which are directly above the leaf (5.3×10^5 FU mm^{-3} and 8.9×10^5 FU mm^{-3} respectively), while L2 and L5, residing on the opposite side of the plant, have much lower fluorescence level (2.3×10^5 FU mm^{-3} and 3.1×10^5 FU mm^{-3} respectively) than L3 and L4 at 30 min (Fig. 7b). CF dye transport is also biphasic but the values within the first 60 min are lower than reported following root application of CF dye (Compare Fig. 7a, b). Alexa-BSA does not show significant improvement in its ability to move into distal leaves following petiole application. Both root and petiole application produce low fluorescence intensities arguing that such a large protein does not move extensively throughout the plant. Alexa-BSA transport is not biphasic but the same orthostichy side leaves with loading site still got higher level of fluorescence, reaches a low peak ($2.6\text{-}5.2 \times 10^5$ FU mm^{-3}) at 60-90 min with little to know protein reaching L5 leaves (0.6×10^5 FU mm^{-3}). Alexa-Histone transport produces values

that are lower following petiole application, than root application but the first peaks are seen in L3 and L4 leaves at 10 (4.2×10^5 FU mm^{-3}) and 30 min ($2.9\text{-}3.9 \times 10^5$ FU mm^{-3}). This is followed by a long plateau. Uptake by L2 leaves is slower and reaches a peak at 60 min.

Fluorescence intensities were examined in stem cross sections (Fig. 7c, d) to determine if the level of fluorescence in the stem over time was at minimally comparable to the fluorescence intensities reported in petioles at 10 min. Cross sections were sectioned through the stem, at a position just below the L1 petiole and measured fluorescence intensities in the vascular rays. Surprisingly, following root or L1 petiole application, the intensities of Alexa-BSA fluorescence in the stems were much higher than those observed in the leaf petioles. There was a linear progression in uptake over 90 min. These data argue that the petiole might function as a clearing house to block entry of certain proteins into leaves.

When comparing stem and petiole fluorescence intensities, it was predicted that similar levels would indicate constant flow into all petioles from the stem. Lower fluorescence in the petioles would indicate reduced fluorescence import into the leaves from the stems suggesting that there is a mechanism regulating transport along the vascular traces diverging from the stem. Higher fluorescence in the petioles than in the stem would indicate that the flow into the petioles would be greater, perhaps due to higher sink strength. Fig. 7c and d show the fluorescence intensities of CF dye, Alexa-BSA, and Alexa-Histone in stem cross sections. The fluorescence intensities at 10 min for all CF dye and proteins were greater than the amounts reported in the petioles at that time regardless of root or petiole application of the compounds. Given that BSA levels

were so low in the aerial parts of the plant, regardless of its delivery into L1 petioles or roots, it is surprised to observe high levels (around 10×10^5 FU mm^{-3} for CF dye and Alexa-Histone, around 6×10^5 FU mm^{-3} for Alexa-BSA) of fluorescence in the stem. Root application delivers the CF dye and proteins more equal to all the vascular bundles than L1 petiole application. That might be due to the cohesion-tension transport play an important role on water transport in xylem. The transpiration of water at the top of the plant develops a large tension (a large hydrostatic pressure), and this tension pulls the high surface tension water up through the xylem.

Vascular rays are configured in a ring around circumference of stem, and it is been noted that all fluorescence appear throughout the central vascular stele (10/12 of all the soil grown-root application experiments), regardless of CF dye or conjugated proteins following root application. However, following L1 petiole application, only some of the vascular rays showed fluorescence, the non-fluorescent rays separate the vascular ring into two or three parts and that engenders discrete fluorescence in the region of the bundle ring of stem transection (10/14 of all the soil grown-petiole application experiments). In addition, the three-segment vascular ring phenomenon (less fluorescence rays than two-segment vascular ring) usually happened to Alexa-BSA but not CF dye or Alexa-Histone . Because the stem cross section where it from is relatively in a higher position compare to where the CF dye or proteins was loaded following root delivery, but it is in a relatively lower position than the L1 petiole, these phenomenon indicates that the CF dye and proteins move downward by L1 petiole delivery to basal stem are less than the CF dye and proteins that move upward from root to basal stem.

Protein transfer to upper leaf petioles of hydroponic *N. benthamiana* plants

To investigate the role of sap flow in protein delivery, plants placed in hydroponic medium would have greater water content and therefore greater flow through the vasculature than plants grown in soil were considered (Li et al., 2002). So it is expected that CF dye, Alexa-Histone, and Alexa-BSA uptake by plants in hydroponic medium would lead to higher fluorescence levels in the petioles than soil grown plants. Table 2 compares the real fluorescence values obtained from petiole cross sections at 10 and 90 min post-delivery of dye and proteins to the plants. Surprisingly, CF fluorescent values are less than 2-fold different among soil and hydroponically grown plants. These data suggest that higher water application does not stimulate CF dye transfer to all petioles. For Alexa-Histone and -BSA at 10 and 90 min following petiole application, uptake was stimulated among hydroponically grown plants delivering 2-5 fold greater fluorescent proteins to all petioles (* represent significant difference between hydro and soil data at $P<0.05$ in table 2), except L3 petiole. For some reason L3 is physiologically different. This pattern of protein delivery was not mimicked in plants where proteins were delivered to the roots. There was 2 to 5 fold increasing in BSA levels in the L1, L3, and L5 petioles following 10 min of root application, but these differences declined over time and there were no real differences by 90 min. These data argue that the flow rates of water through the vasculature enables transfer of dye and proteins through the stem to younger petioles, especially from source leaves but not roots. Petiole application of CF dye and proteins to hydroponic plants still showed higher level of fluorescence intensity in same orthostichy side leaves with loading site as in soil grown experiments (Fig. 8b).

Following root application, the biphasic phenomenon was not observed. CF dye still reached its peak at 30 min post-delivery, and was then keep uptake by plant through 60 and 90 min. Alexa-BSA has equally distribution in all petioles except L4 at 30 min. An obvious peak was shown in Fig. 8a that indicate the L4 uptake BSA more than other petioles did. Alexa-Histone went through a decline between 30-60 min post-delivery (Fig. 7a and 8a) comparing hydroponic data with soil grown data. This decline indicates a unique protein regulation mechanism brought up by hydroponic system, since hydroponic system brought enhanced uptake for Alexa-BSA following petiole application but an opposite effect for Alexa-Histone.

Table 2. Fluorescence intensity for CF dye, Alexa-Histone and Alexa-BSA uptake by *N. benthamiana* petioles at 10 min and 90 min

		Petiole application ($\times 10^5$ FU mm^{-3})				Root application ($\times 10^5$ FU mm^{-3})				
10 min		L2	L3	L4	L5	L1	L2	L3	L4	L5
CF	soil	1.2±0.1	1.6±0.1	0.9±0.3	1.6±0.3	2.1±0.0	1.6±0.4	1.1±0.1*	2.0±0.0	1.1±0.0
	hydro	1.5±0.5	2.6±0.0	4.0±0.5*	1.4±0.2	1.6±0.5	2.0±0.4	0.4±0.0	1.4±0.1	1.1±0.1
Histone	soil	0.7±0.1	3.5±0.3	1.2±0.1	0.2±0.0	5.8±2.0	5.5±1.5	5.3±0.6*	4.9±0.3	2.7±0.6
	hydro	2.0±0.0*	3.3±1.0	2.4±0.0*	1.4±0.3*	5.0±0.1	4.8±0.2	1.9±0.2	2.5±0.1	3.6±0.0
BSA	soil	0.1±0.1	1.0±0.1	0.9±0.1	0.6±0.2	0.2±0.1	0.7±0.1	0.7±0.1	0.7±0.0	0.2±0.1
	hydro	2.2±0.3*	1.5±0.1	2.6±0.2*	1.2±0.0*	1.0±0.0*	1.0±0.0	1.4±0.1	0.9±0.1	1.0±0.1*
90 min										
CF	soil	8.9±0.3	13.5±0.1	14.1±0.1	3.7±0.0	13.1±0.2	13.4±0.1	13.2±0.1	13.8±0.1	13.6±0.0
	hydro	14.4±0.3	14.3±0.1	13.5±0.0	6.4±0.0	12.8±0.1	12.5±0.1	12.9±0.1	13.5±0.3	10.8±0.0
Histone	soil	1.3±0.2	5.5±0.2*	2.4±0.2	0.2±0.1	7.5±0.5	10.8±0.4	10.6±0.5	10.0±0.8	6.7±0.0*
	hydro	2.6±0.4*	1.9±0.3	7.6±0.7*	0.6±0.0*	5.6±1.0	5.4±0.6	5.0±0.1	5.3±0.0	2.7±0.0
BSA	soil	1.5±0.0	5.2±0.8	3.9±0.8	0.6±0.0	1.7±0.2	3.5±0.5	2.7±0.6	2.8±0.3	3.3±0.4
	hydro	4.9±0.5*	7.3±0.2	8.3±0.8*	7.0±0.6*	1.5±0.1	1.7±0.3	3.0±0.0	2.6±0.0	2.4±0.3

CF, Histone and BSA are used for uptaking measurement. There are four application methods for each of CF, Histone and BSA: soil grown, petiole application; soil grown, root application; hydroponic, petiole application and hydroponic, root application.
Fluorescence unit of 10min and 90min uptake by petioles are listed in this table. L1, L2, L3, L4, L5 means the leaf petiole of L1, L2, L3, L4, L5.
Each of the value is the average of the fluorescence unit value of bottom part (branch out from stem) and top part (before reach to leaf) of that exact petiole.
Data are means ± SD (n=4). * represent significant difference between hydro and soil data at $P<0.05$.

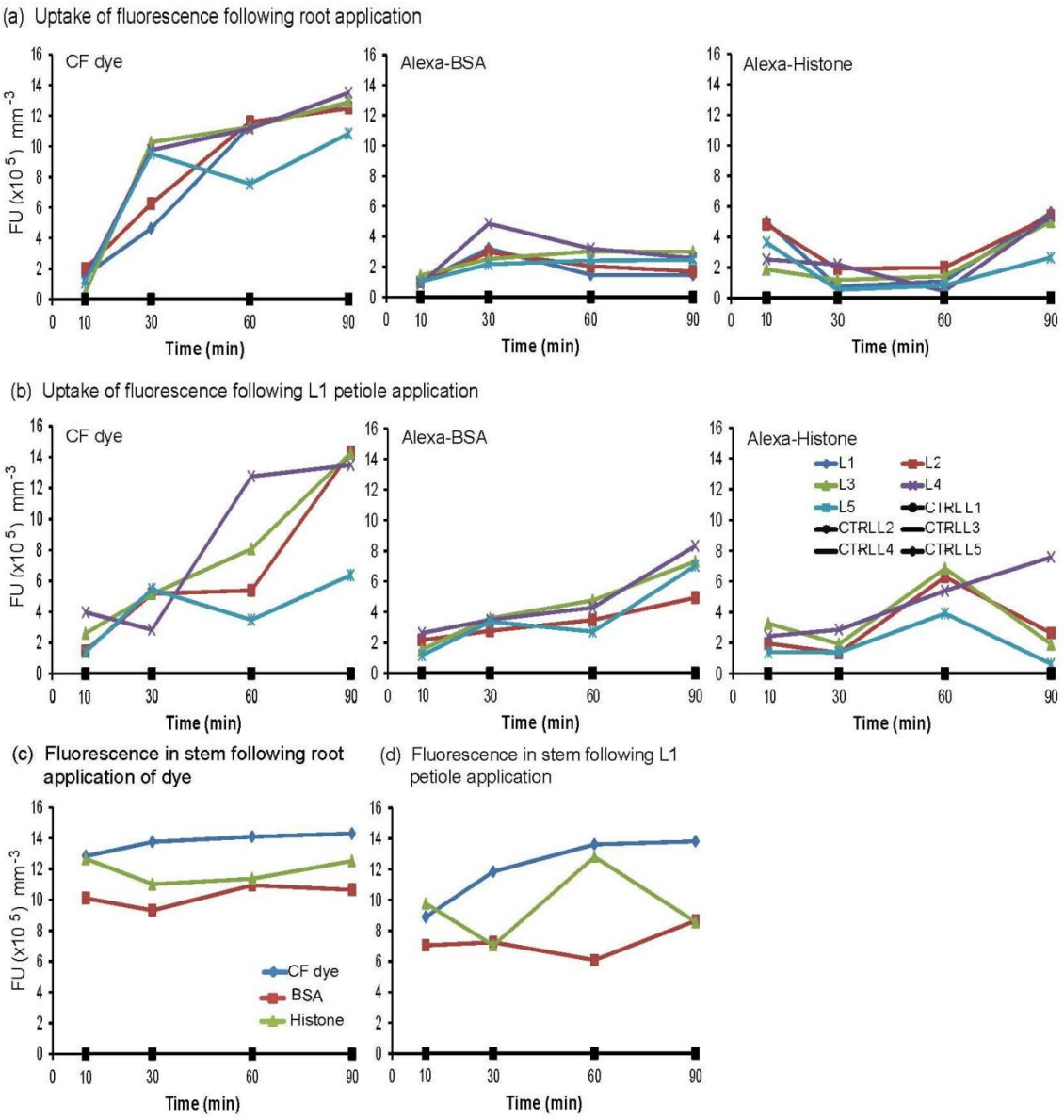

Figure 8. Fluorescence intensity of petiole and stem cross sections of *N. benthamiana* which were transferred to hydroponic system. Graphs depict the average fluorescence values in the central vascular bundles of (n=4) petiole or stem cross sections. The central vascular bundles were selected as ROIs using Image J software and fluorescence values

were recorded. The data were collected at 10, 30, 60 and 90 min after application of CF dye, Alexa-BSA or -Histone.

MRI for measuring Alexa-BSA transfer velocity in *N. benthamiana* stem

MRI can be used as a real-time noninvasive method to study proteins movement in plants. 4.7mg ml^{-1} Gadolinium-diethylenetriamine pentaacetic acid (Gd-DTPA) and 1mg ml^{-1} Biotinyl-bovine serum albumin-gadolinium-diethylenetriamine pentaacetic acid (Gd-BSA) were input into different plants from roots in different *N. benthamiana* plants. Gd-based compound was used as MRI contrast agents, which can improve the visibility of internal body structures in magnetic resonance imaging. First introduced in 1988, Gd-DTPA is used to assist imaging of blood vessels and of inflamed or diseased tissue where the blood vessels become leaky. It is often used when viewing intracranial lesions with abnormal vascularity or abnormalities in the blood-brain barrier in mammalian system experiments. Recently, researchers use it into plant MRI system to assistant Nuclear magnetic resonance research (Donker and Van As, 1999; Gussoni et al., 2001). To investigate the exact transfer velocity of large proteins comparing to fluorescence imaging technology used in previous, Gd-BSA (Towner et al., 2008) was used in the latter MRI experiment to reveal the velocity of movement, comparing to solute like Gd-DTPA.

Fig. 9a, c and d showed the regions of interest (ROIs) circled on the stem which located under leaf 1 petiole but above root system. By comparing signal intensity of different time points to the signal intensity of pre-delivery of Gd-DTPA or Gd-BSA at the same ROIs, results showed that ROIs located longer distance from the root produced later peaks. Gd-DTPA shows signal was transferred to next location and declined in the ROI-2 and ROI-3 (Fig. 9a and b). These data show constant uptake at ROI-1, but the signal moves further away from ROI-2 and -3. ROI-1 represents a reservoir feeding flow to the

next level. ROI-2 and -3 reveal transitions that fail to become saturated with signal. The uptake peaks of ROIs for Gd-BSA delivery were also show further away ROIs peak later pattern from 640s to 1500s in Fig. 9e. But after 1600s, ROI-2 and -3 increased over time while ROI-1 declined. Thus ROI-1 represents a transition rather than a resevoir for protein moving from the root. At 1700 s, it seems that Gd-BSA moved out of ROI-1 and moved into ROI-2 and -3. Protein movement into the region continued to increase whereas dye declines. Perhaps the dye leaked out into adjacent cells, whereas protein remains in the phloem and moved forward through the ROIs.

After calculation using uptake peak as compound arrival to the specific ROI, the velocities for Gd-DTPA movement in *N. benthamiana* stem were obtained, which were 0.077 mm s^{-1} and 0.024 mm s^{-1} for ROI-1 to ROI-2 and ROI-2 to ROI-3 respectively. The velocities for Gd-BSA movement were 0.057 mm s^{-1} and 0.008 mm s^{-1} for ROI-1 to ROI-2 and ROI-2 to ROI-3 respectively. These data indicate the transfer speed for Gd-BSA was slower than Gd-DTPA in stem where under leaf1 branch. And Fig. 9b and e revealed that the initial peak for Gd-BSA uptake in different ROIs were lower than of Gd-DTPA, which was match with the fluorescence imaging data. The velocities in upper plant were also calculated: from ROI3 to the stem between L1 and L2 branch, Gd-DTPA was transferred as a velocity of 0.020 mm s^{-1} while Gd-BSA velocity was 0.007 mm s^{-1}. And from ROI3 to the stem between L2 and L3 branch, the velocity of Gd-DTPA was 0.012 mm s^{-1} while 0.056 mm s^{-1} for Gd-BSA (ROIs not shown in Fig. 9). The velocity of Gd-BSA exceeded Gd-DTPA velocity value, which implied a rapid uptake of Gd-BSA from to stem under L1 to upper portion of plant.

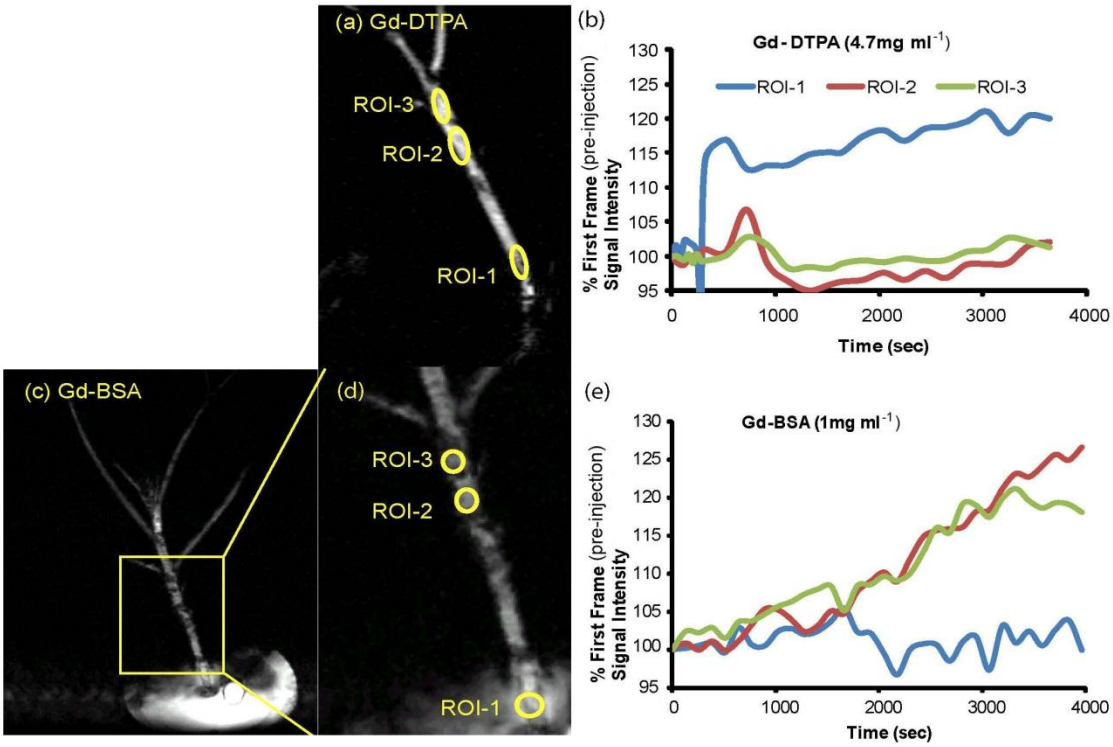

Figure 9. Axial molecular transport in the stem of *N. benthamiana* visualized by MRI by means of the 4.7 mg ml^{-1} Gd-DTPA and 1 mg ml^{-1} Gd-BSA tracer absorbed by the root. (a, c, d) Gd-DTPA or Gd-BSA treated *N. benthamiana* plants. ROI-1 was the point adjacent to stem-root interface. ROI-2 and -3 were points further away from root, below the L1 petiole. (c) Image of whole *N. benthamiana* plant which was treated with Gd-BSA and the yellow box indicates the stem region analyzed in panel (d).

(b, e) Charts show the Gd-DTPA and Gd-BSA signal intensities for each ROI. Values at each time point were normalized with the original pre-injection signal intensity of that ROI. Peaks for ROI-1 precede ROI-2 and -3.

Unloading of CF dye, Alexa-BSA and Alexa-Histone in leaf veins

In *N. benthamiana* leaves, a prominent midrib, or 'class I vein' extends from the petiole to the leaf apex. *N. benthamiana* leaves have the netted vein pattern, smaller veins which have several distinctive vein size classes that branch from the larger veins. Class II veins branch from class I. Class III veins are major veins that branch from class II veins. Class IV and V are minor veins that branch from class III and can be quite small in diameter (Avery, 1933; Ding et al., 1988; Roberts et al., 1997).

After input of CF dye or proteins, the leaves were detached from plant at different time intervals. Fig. 10 shows the unloading of CF dye, Alexa-BSA and Alexa-Histone in veins of L5 at 30 and 90 min post-delivery. In general, CF dye moves into L5 veins along with the veins. Regardless of application methods used, class I, II and III veins of L5 veins of CF dye treated plant became heavily labeled at 30 min (Fig. 10c, o). With time, the fluorescence in class III veins appeared thicker and thicker (Fig. 10a, c, m, o), as though vein contents were diffusing outward (bleeding) (Roberts *et al.*, 1997). This indicates CF dye was unloaded from class III veins into surrounding tissue in sink leaf. Class III veins were the function unloading veins for CF dye in sink leaf.

But Alexa-BSA data showed a different unloading pattern. It did not occur in class III or minor veins at all, but showed discrete fluorescence spots on the leaf lamina (Fig. 10e-h, q-t; Fig. 10e, g, q and s were combined with monochrome images taken at the exact same position to show the existing of class II veins). In Fig. 10e, g, q and s, none of the class III veins were labeled by fluorescence, but there were many fluorescence spots apparent on the leaf. The fluorescence occurring below the epidermal cells or in the epidermal cells was observed by closer examination.

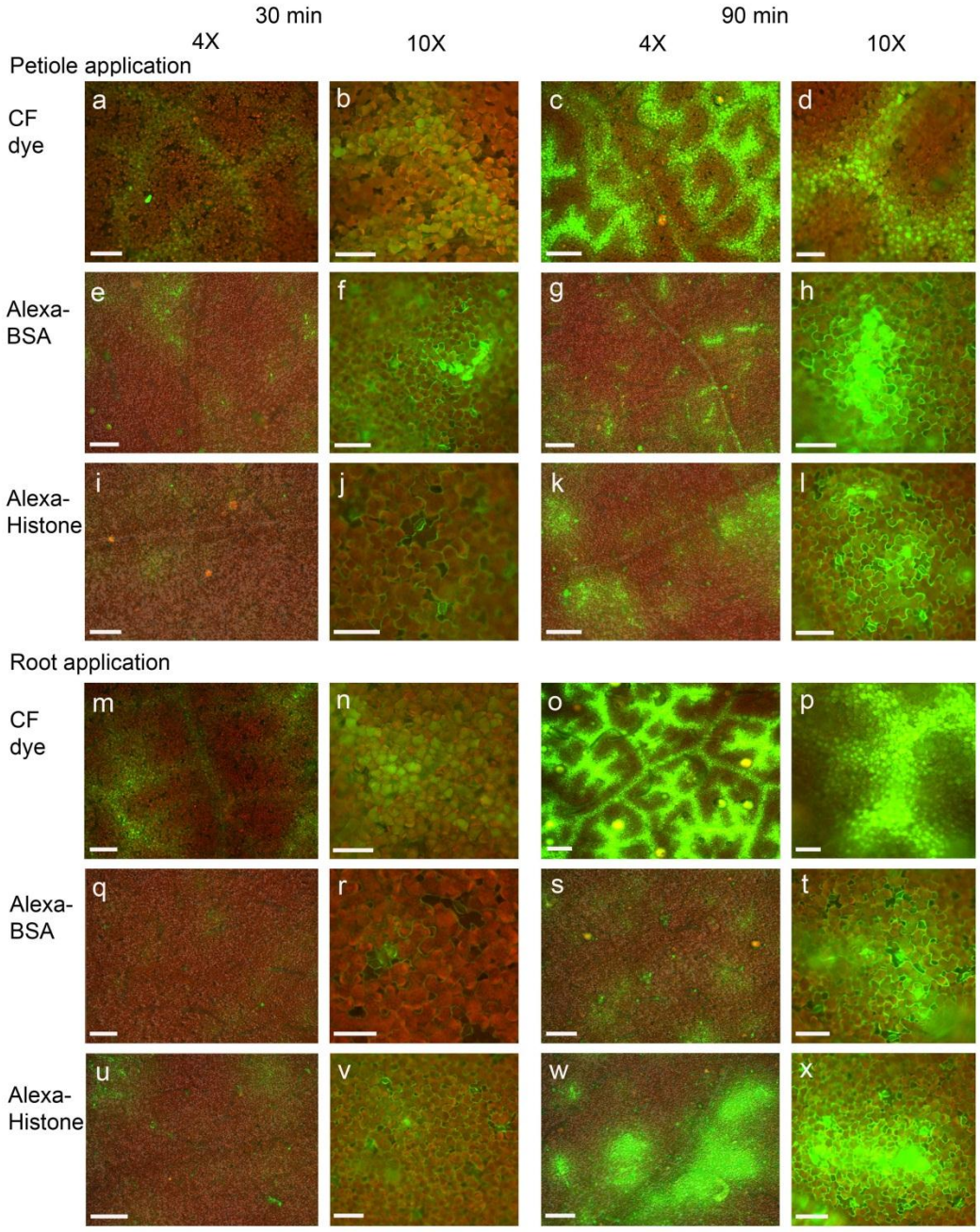

Figure 10. Unloading pattern of CF dye (a-d), Alexa Fluor 488 BSA (e-h) and Alexa Fluor 488 Histone (i-l) in *N.benthamina* L5 sink leaf following L1 petiole application. Unloading pattern of CF dye (m-p), Alexa Fluor 488 BSA (q-t) and Alexa Fluor 488 Histone (u-x) in L5 sink leaf following root application. Images were taken at 30 and 90

min. At 30 min CF dye is mainly inside veins. Fluorescence unloads into neighboring cells at 90 min and produces a "bleeding" pattern around the class II and III veins. Alexa-BSA and Alexa-Histone are seen in leaf lamina, completely unloads from veins. Bars in images taken at 4x magnification = 500 μm; Bars in images taken at 10x magnification = 100 μm.

Fig. 10f shows the fluorescent spots on the leaf, fluorescence margins occur on epidermal cells edge. This implies that after Alexa-BSA was imported into class II vein, they were unloaded from the vein into the surrounding mesophyll cells, which were underneath the epidermal cells. The fluorescence penetrated the epidermal cells and resulted in fluorescence margins of epidermal cells. In some cases, heart-shape regions in Fig. 10f and h, the Alexa-BSA already moved into epidermal cells from the mesophyll cells underneath them. These indicate that the Alexa-BSA went through a complete unloading from veins. There were also some separated fluorescent class III veins of Alexa-BSA treated plants at 90 min (Fig. 10g), telling that the complete unloading of Alexa-BSA was from class III vein. While for Alexa-Histone treated plants, there were no discrete fluorescent class III veins shown regardless the time of post-delivery or application methods used. The fluorescence spots were all near the class II veins (Fig. 10k, w), imply that the complete unloading of Alexa-Histone was from class II veins. Thus, in sink leaves like L5, the functional unloading vein for Alexa-BSA is class III, and the class II is in charge of unloading of Alexa-Histone.

In source/sink transition leaf of CF treated plants (Fig. 11a-d), class III, IV and IV became functional on unloading of CF dye. The fluorescence thickness change in class III is not obvious as fluorescence thickness change of class IV and V (Fig. 11a, b), which indicates the unloading of CF dye from class IV and V veins to surrounding tissues. Class IV and V were not functional as unloading of CF dye when the leaves were check between 10-30 min post-delivery of CF dye in sink leaf (Roberts *et al.*, 1997). These imply that the function of different class veins are depended on the development of vein structures in sink and source leaf they are composed of. With the leaf grow larger in size,

the class IV and V veins become functional on unloading can help photoassimilate reach more area on leaf lamina.

Alexa-BSA images keep showing different unloading pattern like in sink leaf, they did not move into class III or minor veins at all, but showed discrete fluorescence spots on the leaf lamina (Fig. 11e, h and j were edited to show the existing of class III veins). The fluorescence did not move into veins and still show complete unloading pattern. The unloading spots were adjacent to class III veins. The closer examination revealed that the fluorescence occur below epidermal cells for petiole application of Alexa-BSA at both 30 and 60 min since the presence of fluorescent epidermal cell margin. Fig. 11f shows the unloading process from class III vein to surrounding tissue. For Alexa-Histone, the unloading mainly occur in class III at 30 min following petiole application (Fig. 11j) but unloading from class IV and V at 30 min following root application (Fig. 11l, m). These discrete fluorescence spots were splashed all over the leaf lamina, which indicate that the unloading of proteins was not slower than CF dye, but only as a difference pattern. This may be due to there is an active protein export mechanism exist in the leaves of *N.benthamiana* function as clearing system.

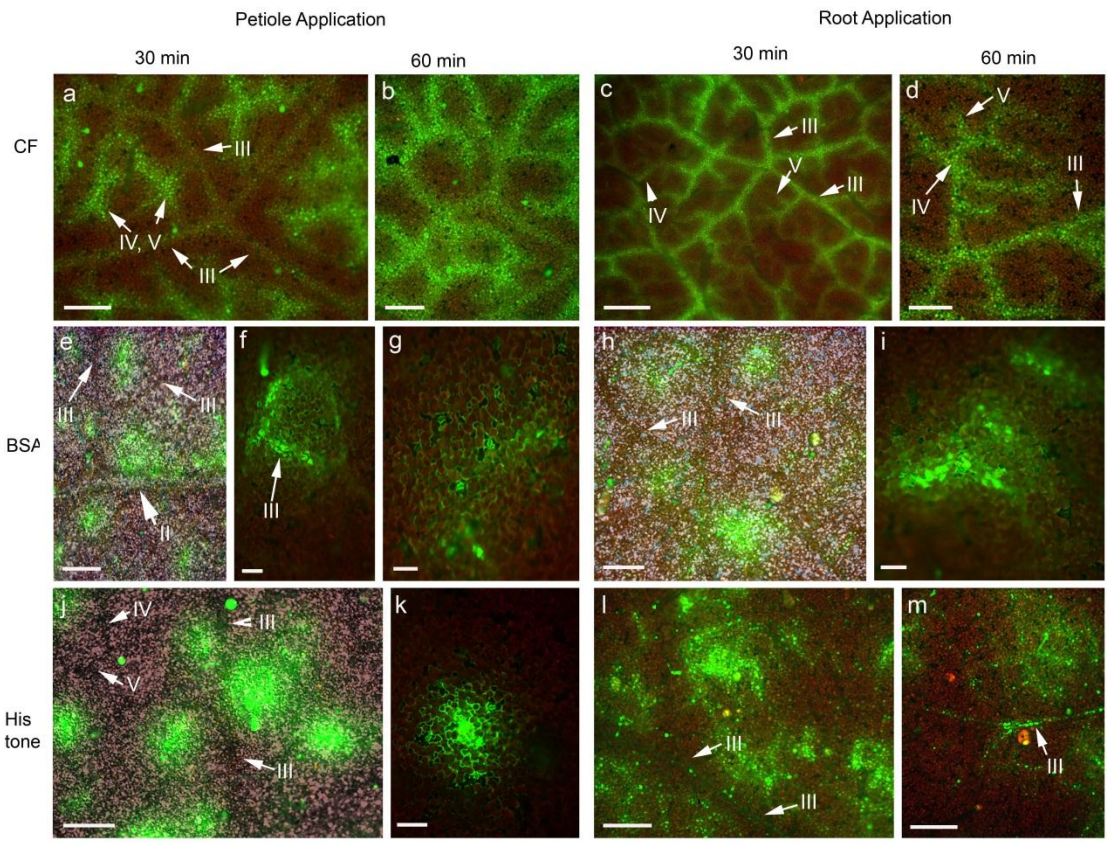

Figure 11. Leaf vascular pattern in L4 source/sink transition leaf following application of CF dye, Alexa -BSA or Alexa -Histone. Images were taken at 30 or 60 min following petiole or root application of fluorescent markers. Class II, III, IV, and V veins are identified in some panels. (e, h, j) are image overlays showing bright field and fluorescent images of veins and fluorescent proteins. Bars in (a, c, e, h, j and l) = 500 μm; Bars in (b, d, f, g, i, k and m) = 100 μm.

Table 3. Initial unloading time point (min) and pattern surrounding unloading veins

	Bottom			Middle			Top		
	L4	L5	L6	L4	L5	L6	L4	L5	L6
L1 petiole application									
CF	60(B)	10(B)	30(B)*	60(B)	90(B)	30(B)*	60(B)	90(B)	30(B)*
BSA	30(CU)	NO	60(B)	30(CU)	30(CU)	60(B)	60(CU)	60(CU)	60(B)
Histone	30(CU)	90(CU)	30(B)	30(CU)	30(CU)	30(B)	30(CU)	30(CU)	60(B)
HCV	90(B)	NO	N/A	NO	NO	N/A	90(B)	30(B)	N/A
Root application									
CF	30(B)	60(B)	N/A	60(B)	60(B)	N/A	60(B)	60(B)	N/A
BSA	90(CU)	90(CU)	30(B)	30(CU)	60(CU)	30(B)	30(CU)	90(CU)	30(B)
Histone	10(B)/ 30(CU)	10(B)	N/A	10(B)/ 30(CU)	10(B)/ 30(CU)	N/A	10(B)/ 30(CU)	30(CU)	N/A
HCV	NO	NO	N/A	90(B)	60(B)	N/A	NO	NO	N/A

B, bleeding
CU, complete unloading
NO, no unloading
N/A, data not available
*, 10 min data not available

Table 3 summarizes the functional unloading veins for CF dye, Alexa-BSA and Alexa-Histone based on our observation in sink or source/sink leaves. These results indicate the different unloading pattern for CF dye and proteins. And the initial unloading time point (min) and pattern surrounding unloading veins were recorded in table 3. As long as there was L6 present, the unloading pattern would be bleeding no matter the CF dye or protein applied or the delivery methods. This indicates that the youngest leaf in *N.benthamiana* plant, the protein regulation system is not ready for use yet. The second result from table 3 is that all the unloading of CF dye show the bleeding pattern while Alexa-BSA (except L6) show the complete unloading pattern no matter which kind of application methods used. But for Alexa-Histone, the complete unloading pattern was only showed in petiole application, while following root application, the bleeding pattern was show at 10 min, then the bleeding pattern became complete unloading at 30 min post-delivery.

Fluorescence intensity in petioles of Fluorescein-HCV treated plants and HCV unloading pattern in leaves

Hepatitis C virus (HCV) is positive-sense single-stranded RNA virus in the family *Flaviviridae*. The HCV particle consists of a core of genetic RNA, surrounded by an icosahedral protective shell of protein, and further encased in a lipid envelope where two envelope glycoproteins-E1 and E2 embedded in. The structural proteins made by the HCV include core protein, E1 and E2; Nonstructural proteins include NS2, NS3, NS4, NS4A, NS4B, NS5, NS5A and NS5B. The virus can remain infectious outside a host for

about 16 days at 25 ℃ and 2 days at 37 ℃. When the temperature drops to 4 ℃ or below, HCV can remain active for more than 6 weeks (Song *et al.,* 2010).

HCV is a major causative agent of chronic hepatitis worldwide (Choo *et al.,* 1989; Saito *et al.,* 1990) and can lead to development of hepatocellular carcinoma (Moriya *et al.*, 1997). The histological features of chronic hepatitis C include bile duct damage, lymphoid follicles and steatosis. The HCV core protein is an unglycosylated protein of about 22 kDa which have genome-packaging function. Typical flaviviral core protein is rich in arginine and lysine, and can bind to RNA genome to form the nucleocapsid of an HCV virion (Santolini, Migliaccio, and La Monica, 1994). It also been reported that the core protein have a regulatory effect on the expression of hepatitis B viral gene (Shih *et al.*, 1993). Although it is localized in cytoplasmic, it shows nuclear translocation when its C-terminal is deleted (Suzuki *et al.,* 1995). The research related to the relationship between HCV protein expression and disease phenotype revealed that HCV core protein plays a direct role in the development of hepatic steatosis (Moriya *et al.*, 1997).

Although HCV is not foodborne disease like hepatitis A virus, it is well-documented as a bloodborne pathogen and is primarily transmitted by injection. In the research using baculovirus-insect cell expression system for HCV protein expression, the results show that HCV core and envelop proteins without p7 were sufficient for viral particle formation (Baumert *et al.,* 1998).

Hepatitis C Virus core antigen [2-192]-Galactosidase-tagged, fluorescein conjugate (Fluorescein-HCV) was input into *N. benthamiana* root or L1 petiole following same methods as Alexa-Histone and Alexa-BSA. The product has a molecule weight of 136kDa which composed of 22kDa HCV core antigen plus 114kDa Galactosidase-

tagged. With such large molecular weight (larger than 34kDa of Alexa-Histone and 66kDa of Alexa-BSA), it is been presumed that Fluorescein-HCV would be taken up by plant at a lower level than Alexa-BSA, but data showed it is not.

Fig. 12a shows the petioles uptake of Fluorescein-HCV following root application. The fluorescence levels reach similar level all petioles at 10 min post-delivery. Petiole of leaf 4 showed biphase uptake pattern with 30-60 min plateau. Petiole of L3 and L1 keep uptaking HCV through all the 90 min, while petioles of L2 and L5 have the uptake peak at 60 min and 30 min respectively. These data indicate the different need of HCV by different petioles, which is distinct from the similar uptake trends of petioles from CF dye, Alexa-BSA and Alexa-Histone treated plants. Although Fluorescein-HCV is large molecular weight protein compare to Alexa-BSA, its uptake by *N. benthamiana* is not in a lower level than Alexa-BSA. Fig. 12a shows all petiole uptake levels of Fluorescein-HCV were higher than of Alexa-BSA at 60 and 90 min post-delivery.

Following L1 petiole application, uptake of Fluorescein-HCV still shows similar orthostichy preferred transfer pattern as CF dye, Alexa-BSA and Alexa-Histone. The L3 and L4 petioles have higher level of uptake than other petioles (Fig. 12b), they were in the same orthostichy side with HCV input site-L1 petiole. It is worthy of notice that the uptake of HCV in L2 and L5 petioles at 10 min post-delivery were in extremely low level and also have a dramatic decline in fluorescence level at 90 min post-delivery. Leaf 2 should be one of the major source leaves in the plant, non-uptake of HCV by L2 petiole indicates Fluorescein-HCV input by L2 is shut off at initial time point. Although Fluorescein-HCV was uptake in a low level at 30 min and 60 min by L2, it still declined

at 90 min, maybe degraded in the petiole after uptake peak. Surprisingly, the low uptake level of HCV in L5 implies that the Fluorescein-HCV is not uptake by sink leaf with time (Fig. 12b). HCV cannot move into sink region similar as PVX (Roberts *et al.*, 1997).

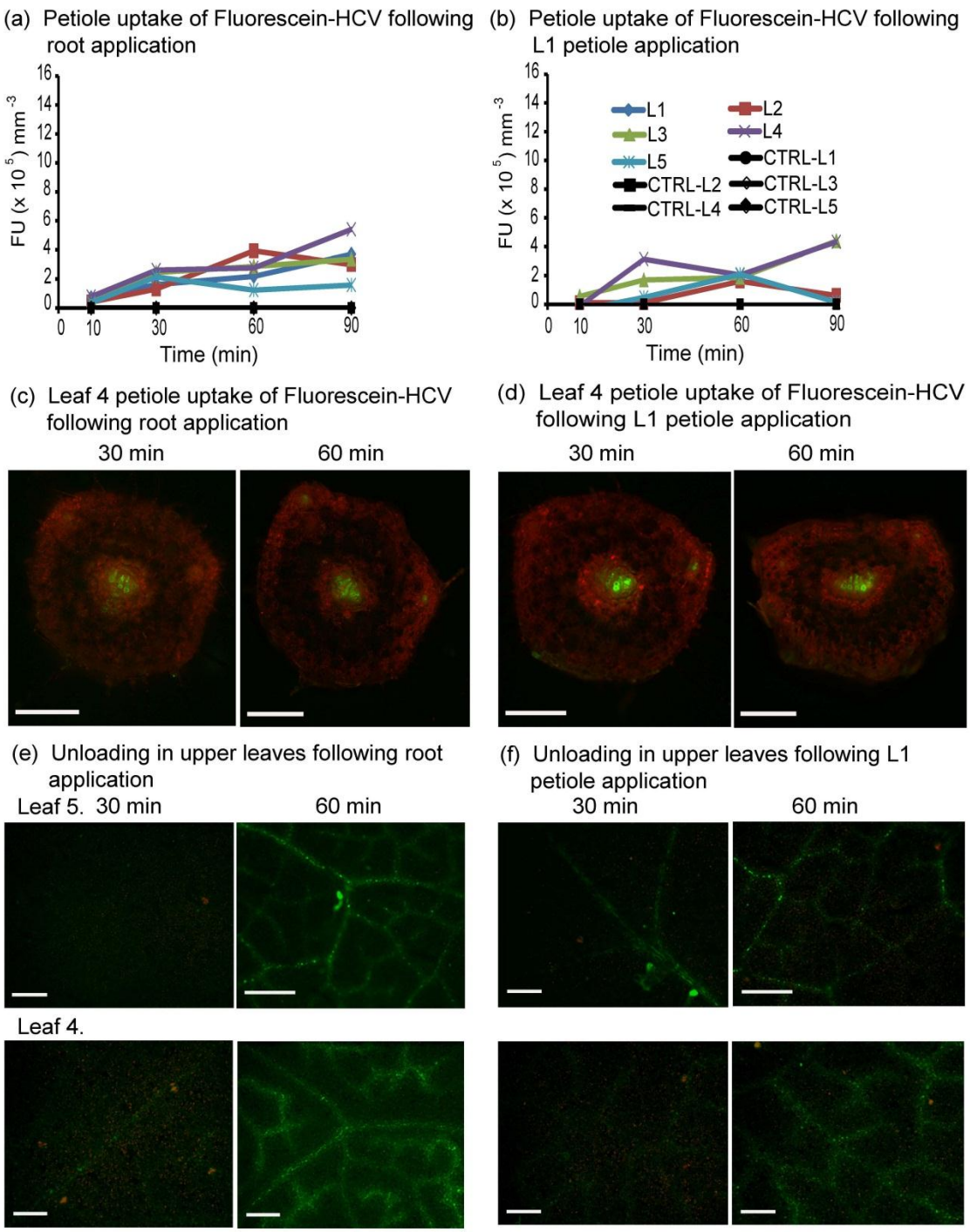

Figure 12. The uptake of fluorescein-HCV core antigen by *N. benthamiana* petioles and leaves.

(a, b) Graphs depict the average fluorescence values in the central vascular bundles of (n=4) petiole sections. The central vascular bundles were selected as ROIs using Image J software and fluorescence values were recorded. The data were collected at 10, 30, 60 and 90 min after application of Fluorescein-HCV

(c, d) L4 Petiole uptake of Fluorescein-HCV following root (c) and L1 petiole (d) delivery at 30 and 60 min. Bars = 500 μm.

(e, f) Leaf vascular pattern in L4 source/sink transition leaf or L5 sink leaf. Images were taken at 30 or 60 min following root or petiole application of fluorescent markers. Bars = 500 μm.

The distribution of Fluorescein-HCV in petiole cross section of *N. benthamiana* shows that the fluorescence was in xylem tracheary element walls (Fig. 12c, d and 13a). This xylem movement is similar to Alexa-BSA (Fig. 6a, b). Fig. 12e and f show the unloading pattern of HCV is similar to CF dye, which is bleeding pattern. But the fluorescence intensity level is low, indicates the unloading of HCV is much slower than CF dye. In both L5 sink leaves and L4 source/sink transition leaves, the unloading occur in class III veins (Fig. 12e, f). Although minor veins function to unload CF dye in L4 source/sink transition leaves, they do not function for Fluorescein-HCV unloading. Interestingly, fluorescence-HCV does not unload from the veins. This is unlike Alexa-BSA or Alexa-Histone suggesting that there is a specific restriction in HCV core antigen movement.

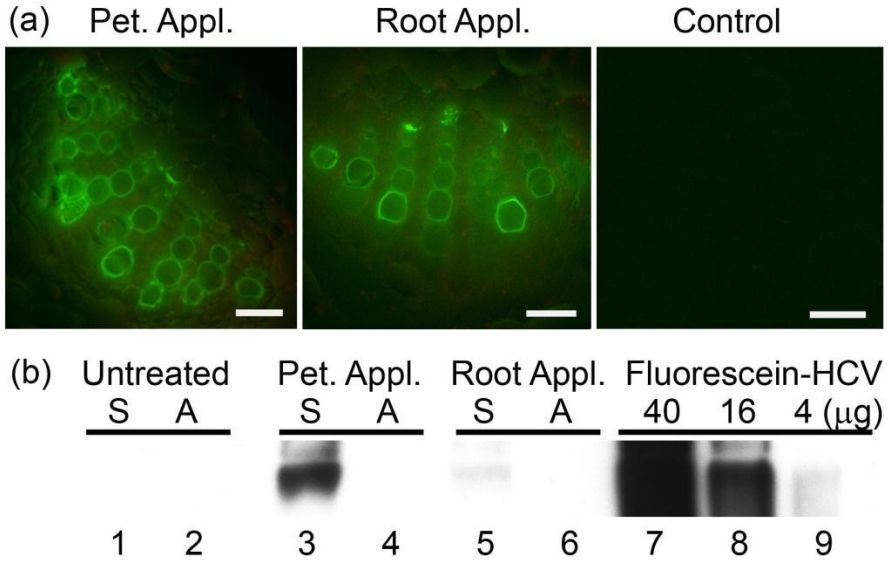

Figure 13. Analysis of symplastic and apoplastic accumulation of Fluorescein-HCV in *N. benthamiana* leaf.

(a) Fluorescence images of Fluorescein-HCV in *N. benthamiana* petiole cross sections following L1 petiole application or root application. Bar = 50 μm. Pet. Appl, petiole application; Root Appl, root application.

(b) Immunoblot probed with monoclonal antisera detecting HCV core protein show accumulation of Fluorescein-HCV core protein at 90 min. Apoplastic wash fluids (A, lanes 2, 4, 6) and cell extracts (S, lanes 1, 3, 5) were pooled from L4 leaves. Fluorescein-HCV in lanes 7, 8 and 9 were directly loaded to gel and produces a band around 136 kDa. Loading amounts (μg) for Fluorescein-HCV are indicated above the lanes.

Fluorescein-HCV did not significantly enter the phloem when it is applied either to the roots or L1 petioles (Fig. 13a). Fluorescence was mainly in xylem tracheary elements. These observations correlate with the low level of trafficking depicted graphically in Fig. 12a and b. On the contrary, Alexa-Histone fluorescence occurring in the phloem, xylem and parenchyma showed relatively high level of trafficking (Fig. 6a, b and 7). Fluorescence did not appear in intercellular spaces suggesting that Fluorescein-HCV follows a symplastic route for long-distance transport. To discover if Fluorescein-HCV was exported to the apoplast, L4 leaves were infiltrated with 2-[N-morpholino] ethansesulfonic acid (MES) buffer and the apoplast wash fluids were pooled. Remaining tissue was ground and both samples were analyzed by SDS-PAGE and immunoblot (Fig. 13b). Results showed Fluorescein-HCV was mainly in tissue extracts and not in the apoplastic wash fluids. And the existing amounts of Fluorescein-HCV were different in the L4 of L1 petiole application and root application plants. Although same amount of Fluorescein-HCV (36 μg) was loaded into L1 petiole or root, Fig. 13b shows there was about 10 μg Fluorescein-HCV exist in L4 of L1 petiole application plant and about 3 μg in L4 of root application *N. benthamiana*. As we known, following the L1 petiole application, the Fluorescein-HCV was only loaded into several bundles belong to L1 petiole. While following root application, all the bundles of root then stem were able to access the Fluorescein-HCV. Interestingly, the bundles of L1 petiole can transport the Fluorescein-HCV along bundles of stem into petiole of L4. These data suggest a sorting mechanism in the stem vasculature.

Measuring of fluorescence intensity in petioles of CF dye, Alexa-BSA and Alexa-Histone treated *B. oleracea* plants

Plants in *Brassica* family, with close relationship to the fully sequenced model plant *Arabidopsis thaliana*, are employed for studying phloem biology because there are large numbers of vascular bundles throughout the stem and this enables researchers to collect significant volumes of phloem sap for proteomic studies (Giavalisco *et al.*, 2006). Several classes of proteins involved in growth and metabolism have been reported in the phloem sap but little is known about their transport and unloading into various organs where they might function (Buhtz et al., 2008; Giavalisco et al., 2006).

In this study, *B. oleracea* plants were used to assess whether the arrangement of vascular bundles in the leaf petioles is a factor in the rate and quality of mass flow from the stem into the leaf. Leaves are numbered L1 to L5 in their order of emergence above the soil, L1 is the mature source leaf that lies closest to the soil surface and L5 is the youngest sink leaf to emerge. The *B. oleracea* petiole is triangular in shape and has a single U-shaped layer of collateral vascular bundles (Fig. 1b). *B. oleracea* has two classes of vascular bundles in the petiole. There are usually three to four large fan-shaped bundles (Fig. 1d, 14a, 14b arrows with tail) found in all leaf petioles, and this does not vary with leaf maturation. There are two to seven smaller circular bundles (Fig. 14a, b arrows without tail) per cross section and these vary in number with maturation. In L3-L5 leaf petioles, it is noted that the numbers of circular bundles varied between four and seven. In L1 and L2 leaf petioles there were between two and four circular bundles. The phloem occurs on the abaxial side of the xylem (Fig. 1d).

Commercially available CF dye (60 μg ml^{-1}), Alexa-BSA and Alexa-Histone H1 (0.3 mg ml^{-1}) were applied to either the L1 petiole (Roberts *et al.*, 1997) or roots of *B. oleracea* plants. Importantly the concentrations of dye and protein that were used in this study produced similar absorbance values. In reports when CF dye is applied to the cut L1 petiole, the dye follows the same route as photoassimilates and unloads in sink leaves (Roberts *et al.*, 1997). On occasions CF dye enters the xylem (Roberts *et al.*, 1997).

To record CF dye and proteins transfer to the upper leaves of *B. oleracea* plants, 0.5 mm sections were cut from the petioles of each upper leaf at 10, 30, 60, and 90 min. Digital images of the cross sections were recorded using epifluorescence microscopy (Fig. 14a, b). The pattern of fluorescence was specific to the dye or proteins applied to the plant. The average FU mm^{-3} of fan shaped bundles and circular bundles were calculated and shown in Table 4. For CF dye, all vascular bundles, regardless of their dimensions showed similar fluorescence intensities when dye was applied to the L1 petiole or the root (Fig. 14a, b). The average values (FU mm^{-3}) of fluorescence in fan shaped bundles and circular bundles among L5 petioles when dye was applied to the L1 petiole were similar at each time point (Table 4). At 90 min, the values reached a maximum at 6.4×10^5 and 8.8×10^5 FU mm^{-3}. When CF dye was applied to the roots, the average values for fan shaped and circular bundles also reached similar maximums of 4.1×10^5 and 3.9×10^5 FU mm^{-3} at 90 min. These data indicate that CF dye is similarly distributed among all vascular strands.

For Alexa-BSA fluorescence appeared to be concentrated in the xylem and the values in fan shaped and circular bundles were lower than CF dye. The average fluorescence value at 90 min for the fan shaped bundles was 0.8×10^5 FU mm^{-3}, which

was greater than 0.4 $\times 10^5$ FU mm^{-3} for the circular bundles (Fig. 14b and Table 4) following L1 petiole application. The values following root application were higher than following L1 application. The average fluorescence value at 90 min for the fan shaped bundles was 3.4×10^5 and for circular bundles was 1.5×10^5 (Table 4). For Alexa-Histone, fluorescence spread throughout the fan shaped vascular bundles and was not restricted to the xylem (Fig. 14 and Table 4). The average fluorescence values were lower for Alexa-Histone than -BSA following L1 petiole application, but higher following root application. The average fluorescence value at 90 min for the fan shaped bundles was 0.1×10^5 FU mm^{-3}, and for circular bundles was 0.2×10^5 FU mm^{-3} following L1 petiole application. The average fluorescence value at 90 min for the fan shaped bundles was 2.8×10^5 FU mm^{-3}, and for circular bundles was 1.2×10^5 FU mm^{-3} following root application (Fig. 14b and Table 4). These data suggest that there is greater protein movement in L5 petiole when they are added to the roots than petioles. Movement following root application was higher for proteins in the fan shaped vascular bundles while CF dye appears to be equally distributed among the vascular bundles.

Fluorescence in petiole cross sections was recorded by measuring the fluorescence intensity of three fan-shaped bundles and two circular bundles in L5 petiole cross sections using ImageJ software. These values were summed and then the averages among petiole cross sections (n=4) FU were plotted relative to time (Fig. 14c, d). Movement of CF dye, Alexa-BSA, or Alexa-Histone from the site of application in the L1 petiole to L5 sink leaves was slow. The plots show CF dye accumulation in L5 vascular strands was generally higher than Alexa-BSA or Alexa-Histone (Fig. 14a, c). The plots also show higher levels of CF dye or proteins at 30 min (1.5 to 4.7×10^4 FU) in

the L5 petiole after they were applied to plant roots (Fig. 14d). The CF dye values continued to increase until 90 min (9.4×10^4 FU). Alexa-BSA values reached a plateau between 30 and 60 min (around 1.5×10^4 FU) followed by a second phase of Alexa-BSA transfer into the petiole that reaches a new maximum at 90 min (5.2×10^4 FU). Alexa-Histone values kept a plateau around 4.1×10^4 FU (Fig. 14d).

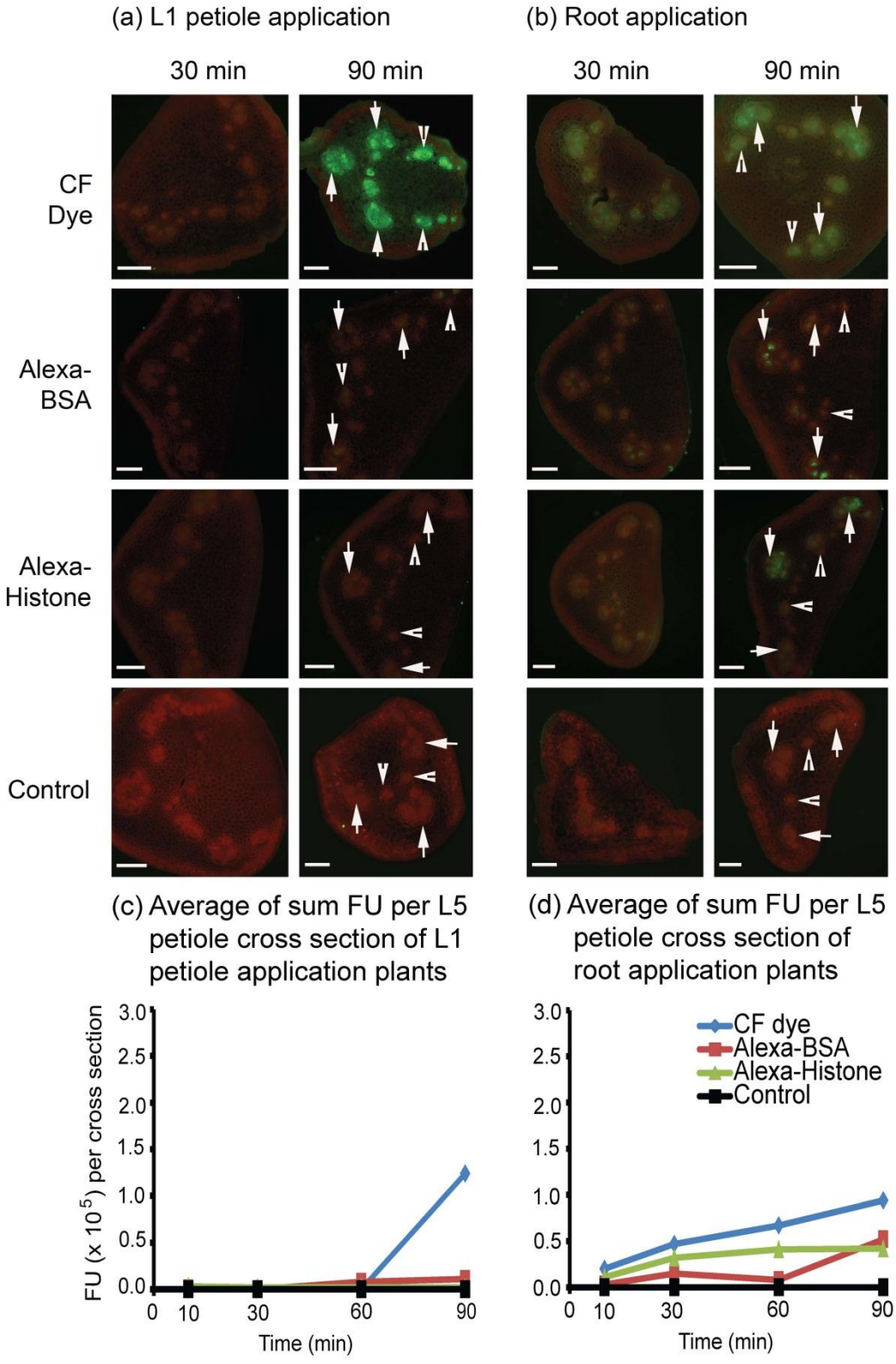
(a) L1 petiole application
(b) Root application
30 min
90 min
30 min
90 min
CF Dye
Alexa-BSA
Alexa-Histone
Control
(c) Average of sum FU per L5 petiole cross section of L1 petiole application plants
(d) Average of sum FU per L5 petiole cross section of root application plants
FU (x 10^5) per cross section
3.0
2.5
2.0
1.5
1.0
0.5
0.0
0
10
30
60
90
Time (min)
CF dye
Alexa-BSA
Alexa-Histone
Control

Figure 14. Images of L5 petiole cross sections of *B. oleracea*. Images show the fluorescence intensity of L5 petiole cross sections (n=4) following L1 petiole (a) or root (b) application at 30 and 90 min. Plants were treated with CF dye, Alexa Fluor 488 BSA and Alexa Fluor 488 Histone H1. Bar = 500 μm. (c, d) Three fan-shaped (arrows) and two circular bundles (arrowheads) per cross section values were summed and then the averages among petiole cross sections FU (two petiole cross sections were used for each petiole, which were sections at top and bottom part of each petiole) (n=4) were presented in the charts. CF dye reaches a maximum at 90 min, although the uptake levels were low at 30 and 60 min. Uptake of Alexa-BSA is low delivered to the L1 petiole, but increased when delivered to root. The amount of Alexa-Histone that transfers to L5 petioles reaches saturation and a plateau at 30 min following root delivery.

Table 4. Average FU per mm^3 of fan shaped and circular bundles of L5 petiole at different time points. ($\times 10^5$ FU mm^{-3})

		Fan shaped bundles			Circular bundles		
		30 min	60 min	90 min	30 min	60 min	90 min
Soil-petiole Appl.	CF dye	0.0 ±0.0	0.0 ±0.0	6.4 ±1.3	0.1 ±0.1	0.1 ±0.1	8.8 ±2.5
	Alexa-BSA	0.2 ±0.2	0.1 ±0.1	0.8 ±0.4	0.2 ±0.2	0.9 ±0.2	0.4 ±0.4
	Alexa-Histone	0.2 ±0.0	0.2 ±0.1	0.1 ±0.1	0.1 ±0.1	0.1 ±0.1	0.2 ±0.2
Soil-root Appl.	CF dye	2.6 ±1.8	4.6 ±0.9	4.1 ±1.7	2.6 ±0.6	4.4 ±1.6	3.9 ±1.9
	Alexa-BSA	0.8 ±0.4	0.2 ±0.2	3.4 ±1.3	1.1 ±0.1	0.9 ±0.1	1.5 ±1.1
	Alexa-Histone	2.4 ±1.4	2.7 ±1.0	2.8 ±0.1	0.8 ±0.4	2.1 ±0.9	1.2 ±0.5

Protein transfer to upper leaf petioles of soil grown *B. oleracea* plants

The transport of CF dye, Alexa-BSA and Alexa-Histone was monitored at 10, 30, 60, and 90 min post-delivery in cross sections of L1-L5 petioles. Control plants were treated with buffer only. Fluorescence in petiole cross sections was sampled by measuring the fluorescence intensity of three fan-shaped bundles and two circular bundles in L5 petiole cross sections using ImageJ software. These values were summed and then the averages among petiole cross sections (n=4) FU were plotted relative to time (Fig. 15). By measuring the total FU per cross section in each leaf petiole, the destinations of the exogenously applied dyes and proteins can be identified.

Fig. 15 shows the average of total FU per petiole or stem cross section of soil grown *B. oleracea* plants. Following root application of CF dye and Alexa-Histone, fluorescence increased linearly over 90 min into most petioles, but for L2-L4 there was generally a peak in fluorescence around 30 min. The values ranged from 0.1-1.0 $\times 10^5$ FU. The values for Alexa-BSA and -Histone also remained low, 0.1-0.5 $\times 10^5$ FU. Alexa-BSA fluorescence reached a low peak at 60 or 90 min in each leaf petiole, which was delayed relative to CF dye. Interestingly the mature L1 and L2 petioles showed higher accumulation of Alexa-BSA fluorescence than the younger sink petioles. These data suggest that the pattern of Alexa-BSA movement into leaves is not like CF dye. Alexa-Histone also reached a low plateau for most petioles between 30 and 60 min. In general dye and protein movement from the roots was low.

Following L1 petiole application, CF dye accumulation in mature L2 and L3 petioles increased between 30 and 90 min, while sink L4 and L5 petioles showed accumulation increasing between 60 and 90 min (Fig. 15b). The values for Alexa-BSA

and -Histone remained low, 0.1-0.5 $\times 10^5$ FU, as reported following root application. The data suggest that protein movement was low in soil grown plants regardless of delivery to roots or L1 leaf petioles and was unlike CF dye transfer through the phloem (Fig. 15b). Fluorescence in stem cross sections was also examined. Cross sections were taken below the L1 petiole to determine if transfer through the stem was impeded. Following root or L1 petiole application of dye, Alexa-BSA or Alexa-Histone, fluorescence was 10 to 15-fold higher than the values in the petioles (Fig. 15c, d). These data indicate that there is significant amount of dyes and proteins moving through the stem but these are partitioned at the petiole with much less flowing into the leaves.

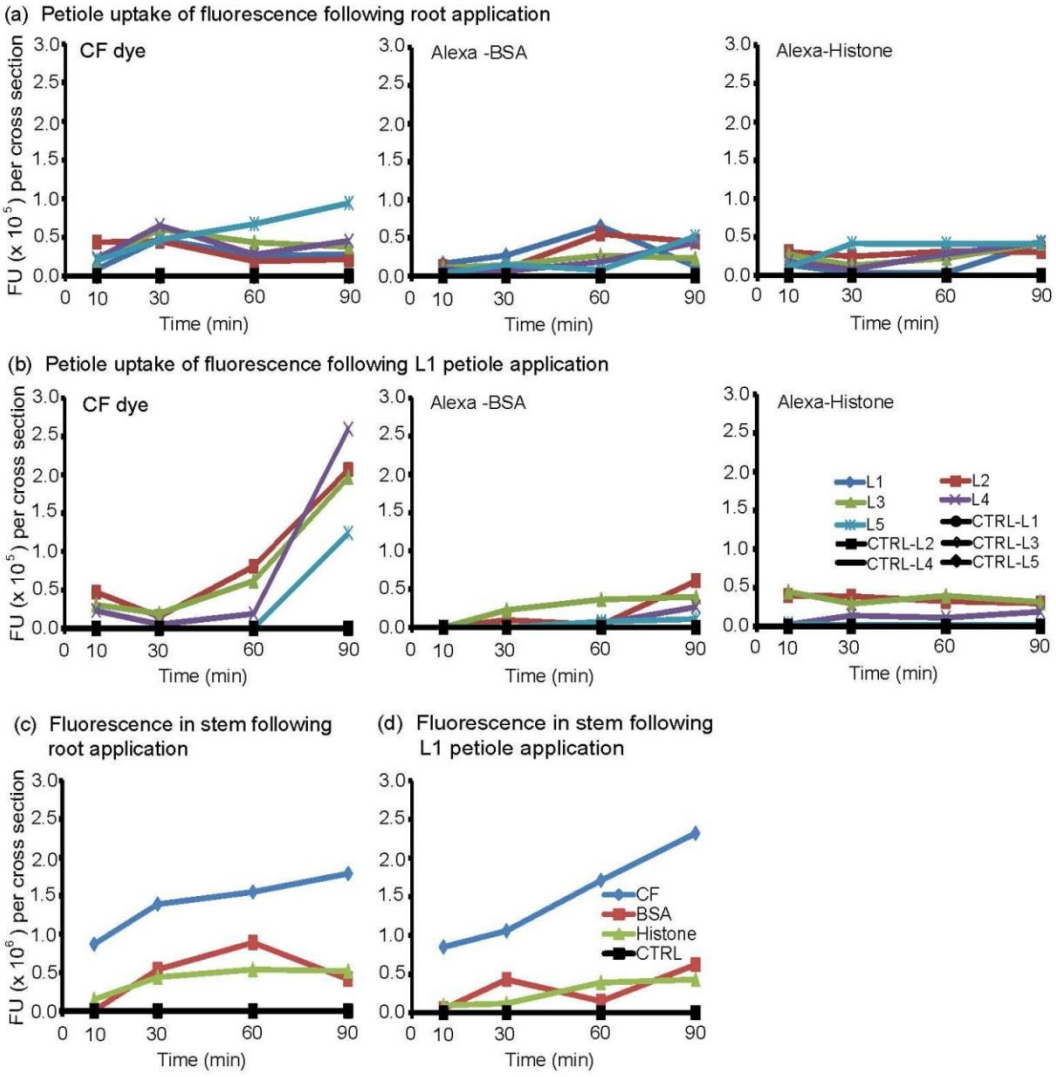

Figure 15. Total fluorescence unit per petiole and stem cross section of soil grown *B. oleracea*. Three fan shaped and two circular bundles per cross section values were summed and then the averages among petiole cross sections FU (two petiole cross sections were sliced for representing intensity of each petiole, which were section at top of petiole and bottom of petiole; n=4) were presented in the charts. The vascular bundles were selected as ROIs using ImageJ software and fluorescence values were recorded. The data were collected at 10, 30, 60 and 90 min after application of CF dye, Alexa-BSA or -Histone.

Protein transfer to upper leaf petioles of hydroponic *B. oleracea* plants

To investigate the effect of water content to CF dye and protein uptake in *B. oleracea*, soil grown *B. oleracea* plants were transferred into hydroponic bags 24 h before applying the dyes or proteins to the plants. The first observation following delivery of dyes or proteins to the roots is that fluorescence is distributed to all leaf petioles. Fig. 16a shows that CF dye accumulates to higher levels in young leaves than mature leaves, but there is a general linear increase in fluorescence between 10 and 90 min. Alexa-BSA had two phases of increased fluorescence. The first phase was between 0 and 30 min which was followed by a decline and then a second phase between 60 and 90 min. Alexa-BSA was distributed to all petioles (Fig. 16a). Alexa-Histone showed a linear increase in fluorescence accumulation over time in all petioles, similar to CF dye. Alexa-Histone showed higher fluorescence in mature leaves than sink leaves at 90 min (Fig. 16a). These data indicate that the pattern of dye and protein movement from the roots to leaves is driven by phyllotaxy.

Following L1 petiole application, CF dye accumulation increased in two phases. The first peak in fluorescence was at 10 min with fluorescence reaching 1.2-1.5 $\times 10^5$ FU (Fig. 16b). The second phase was 30-60 min which was earlier than in root application (Fig. 16a). Fluorescence in leaf petioles due to Alexa-BSA showed a linear increase over time, although the levels remain lower than CF dye (Fig. 16b). The uptake of Alexa-Histone following L1 petiole application reached a plateau between 30 and 60 min (Fig. 16b). The level of Alexa-Histone was higher than Alexa-BSA but lower than CF dye. The fluorescence intensities in stem cross sections of plants maintained in the hydroponic media was 10 to 15-fold higher than in the leaf petioles (Fig. 16c, d). CF dye

fluorescence was consistently higher than Alexa-BSA or -Histone. The fluorescence intensity due to the proteins in the stem reached 0.5×10^6 FU during 0-60 min, but the intensity in petiole cross sections was lower at 1.5×10^5 FU. These data indicate that dye and proteins import into the leaves is regulated along the vascular which branch from the stem.

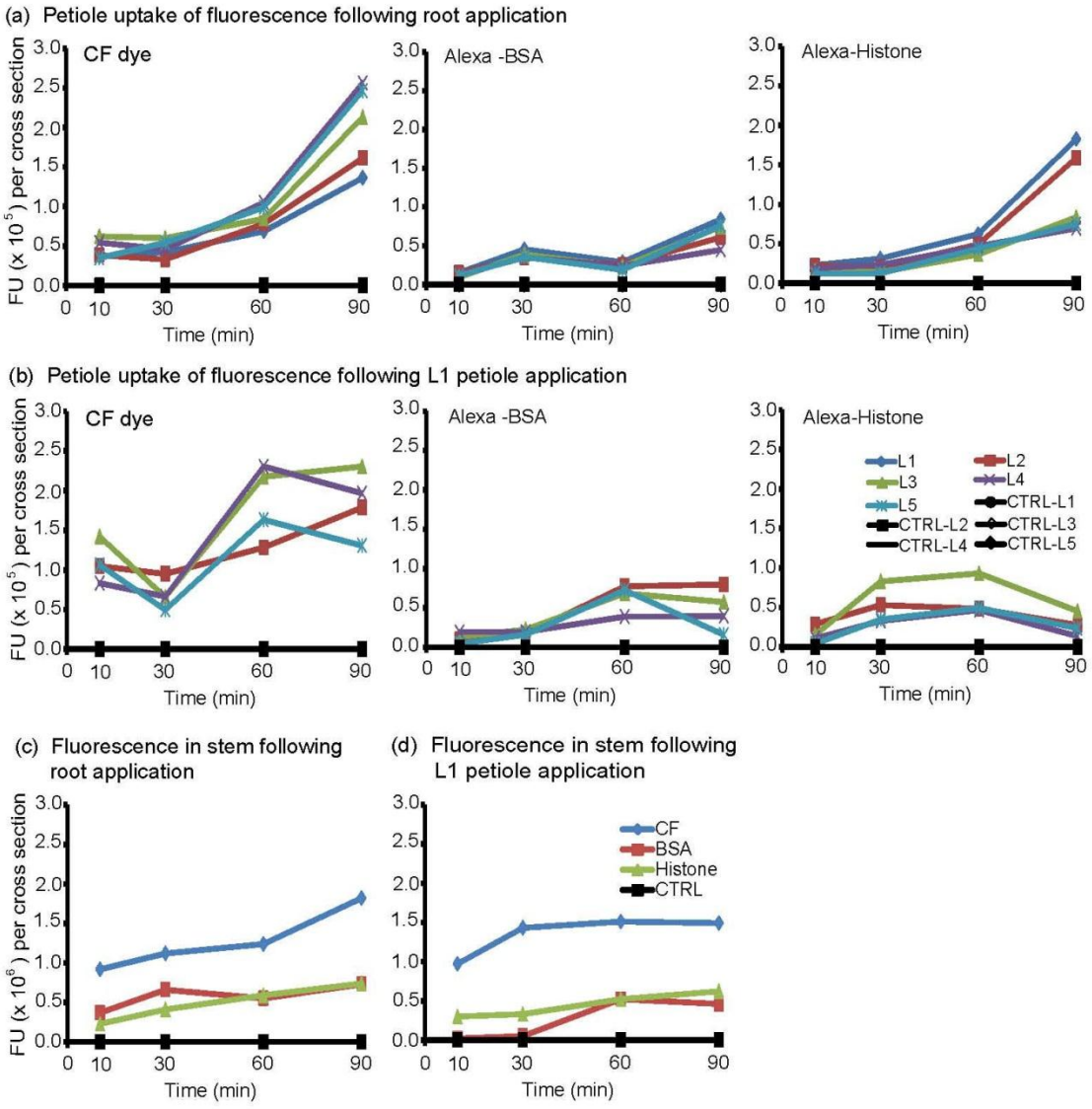

Figure 16. Total fluorescence unit per petiole and stem cross section of hydroponic *B. oleracea* plants. Three fan shaped and two circular bundles per cross section values were summed and then the averages among petiole cross sections FU (two petiole cross sections were sliced for each petiole, section at top of petiole and bottom of petiole) (n=4) were presented in the charts. The vascular bundles were selected as ROIs using ImageJ software and fluorescence values were recorded. The data were collected at 10, 30, 60 and 90 min after application of CF dye, Alexa-BSA or -Histone.

Unloading of CF dye, Alexa-BSA and Alexa-Histone in *B. oleracea* leaf veins

The class I vein in *B. oleracea* leaves is also called the midrib and extends from the petiole to the leaf apex. The netted vein pattern is similar to *N. benthamiana* leaves, with smaller vein classes that branch from the larger veins. Class III veins are major veins that branch from class II veins. Class IV and V are minor veins that branch from class III and can be quite small in diameter (Avery, 1933; Ding et al., 1988; Roberts et al., 1997). After dye or fluorescent proteins were applied, the leaves were detached from plant at various times for observation. Fig. 17 shows the unloading patterns produced by CF dye, Alexa-BSA and Alexa-Histone fluorescence in L5 and L4 at 30 and 90 min.

Regardless of whether CF dye was applied to the roots or L1 petiole, fluorescence was seen in class III, IV and V veins of L5 and L4 90 min (Fig. 17a, d). Following L1 petiole application, CF dye was first seen in the leaves at 90 min. Following root application of CF dye to *B. oleracea* plants, fluorescence was seen in the leaf veins at 30 min, indicating early transfer than when the dye is applied to the petioles (Fig. 17d). In both cases, CF dye appeared to bleed into the mesophyll from class IV and V veins (Fig. 17a), indicating that CF dye unloads from minor veins (Fig. 17a2, a4, d2, d4).

Alexa-BSA was seen in the major veins following L1 petiole application but reached all minor veins following root application at 90 min in L4 and L5 leaves (Fig. 17b, e). Alexa-BSA was not apparent in the minor veins at 30 min but can be seen at 90 min, suggesting that there is a sorting mechanism that delays protein movement into these veins (Fig. 17b, e).

There were some differences in the vascular unloading pattern in leaves treated with Alexa-BSA. At 90 min following L1 petiole application, fluorescence accumulated in class III veins as well as the stomata of L4 leaves (Fig. 17b4, g). In root application images, Alexa-BSA fluorescence produced different leaf patterns in L4 and L5 leaves. In L5 leaves, Alexa-BSA was mainly in veins (class II-V, Fig. 17e2) while in L4 leaves fluorescence was seen in epidermal cells and stomata (Fig. 17e4, i). One explanation is that L5 leaves were quite young and the vasculature was restrictive with respect to protein unloading.

Following petiole application of Alexa-Histone, fluorescence was seen in leaf veins of L4 but not L5 veins at 90 min. However, following root application of Alexa-histone, fluorescence was seen in the L4 and L5 leaf veins and lamina at 30 min (Fig. 17c, f). Thus Alexa-histone does not have the mobility through the phloem as Alexa-BSA of CF dye following petiole delivery. Alexa-Histone coalesces in patches along the leaf lamina surrounding stomata, especially in leaf 2. The distribution within the leaf lamina was unlike Alexa-BSA. Future experiments will determine if apoplast and symplast unloading plays a role in the distribution of proteins in the leaf.

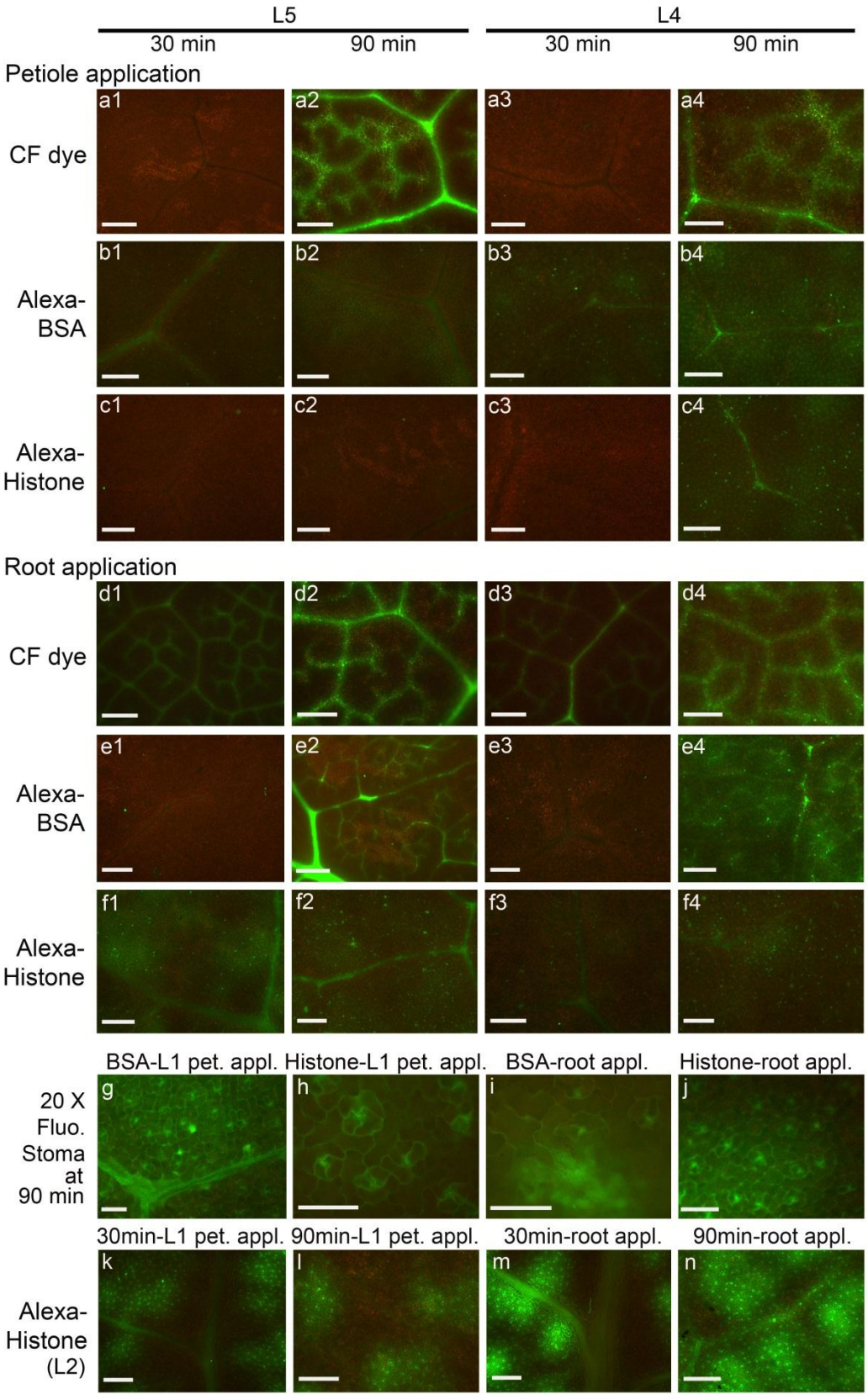
L5
L4
30 min
90 min
30 min
90 min
Petiole application
CF dye
Alexa-BSA
Alexa-Histone
Root application
CF dye
Alexa-BSA
Alexa-Histone
BSA-L1 pet. appl.
Histone-L1 pet. appl.
BSA-root appl.
Histone-root appl.
20 X Fluo. Stoma at 90 min
30min-L1 pet. appl.
90min-L1 pet. appl.
30min-root appl.
90min-root appl.
Alexa-Histone (L2)

Figure 17. Unloading pattern of CF dye, Alexa Fluor 488 BSA and Alexa Fluor 488 Histone H1 in *B. oleracea* upper leaves following L1 petiole application and root application.

(a-c)Unloading of CF dye, Alexa Fluor 488 BSA and Alexa Fluor 488 Histone H1 in L5 and L4 following L1 petiole application. Bar = 500 μm.

(d-f)Unloading of CF dye, Alexa Fluor 488 BSA and Alexa Fluor 488 Histone in L5 and L4 following root application. Bar = 500 μm.

(g-j)Enlarged fluorescent stoma of unloading Alexa-BSA following L1 petiole application (g) and root application (i), Alexa-Histone following L1 petiole application (h) and root application (j) at 90 min. Bars in images taken at 20 x magnification=100 μm.

(k-n)Unloading of Alexa Fluor 488 Histone H1 in L2 following L1 petiole application at 30 min(k) and 90 min (l), and following root application at 30min (m) and 90min (n) post-delivery. Bar = 500 μm. Although Alexa-BSA shows unloading through stomata, all the leaves exhibit similar intensity of fluorescent stomata. While unloading of Alexa-Histone reveals specific stomata unloading leaf, which is L2.

CHAPTER IV

CONCLUSIONS AND DISCUSSION

Four different sized fluorescent molecules: CF dye (460 Da), Alexa-Histone (34 kDa), Alexa-BSA (66 kDa), and Fluorescein-HCV (136 kDa) were used to study transfer from loading site in the roots and L1 petiole to the upper leaves of *N. benthamiana*. CF dye and Alexa-Histone were found to be capable of moving throughout the plant vasculature following root application. In contrast, the fluorescence intensity levels were relatively low in petioles of Alexa-BSA and Fluorescein-HCV treated *N. benthamiana*, which indicates minimal movement (Figs. 7, 8, and 12).

The results from different application methods indicate the CF dye and fluorescent proteins are transported to different destinations. In soil grown *N.benthamiana* plants, root applied proteins show predictable toward-sink movement (Fig. 7a). But, L1 petiole applied CF dye and proteins are not always supplied to the sink leaves. No matter if it is soil grown plant or hydroponic plant, the leaves at the same orthostichy side of loading site gain more CF and proteins following L1 petiole application (Fig. 7b and 8b). Intriguingly, the sink leaf preferred transport of CF and

fluorescent proteins in soil grown plants can be disturbed by hydroponic system (Fig. 7a and 8a).

No matter which application methods were used, CF dye shows biphasic transport. Uptake of Alexa-Histone also shows this pattern except L1 petiole application in soil grown *N. benthamiana* plants. But Alexa-BSA only show biphasic uptake in soil grown plants following root application, and neither rate of two phase reach to the level of CF and Alexa-Histone. If only check the first uptake phase that occurs within 10 min post-delivery, it is interesting to note that the initial transfer of Alexa-Histone is rapid although it is larger than CF dye. This indicates that protein size relative to CF dye is not the defining feature for the initial uptake phase. Since Alexa-Histone was only recovered in symplastic samples, apoplastic transport is not a positive factor for long distance movement of Alexa-Histone. Another finding is that when Alexa-Histone was applied to the L1 petioles its movement was reduced during first 10 min in comparison to the fluorescence intensity in root application. These observations are harder to explain. Perhaps the vascular dimensions of the L1 petiole are different than from the roots and this changes the transfer potential or rate to distal parts of the plant. Or the vascular trace connecting the L1 petiole and stem down regulates the rate export from the leaf in comparison to phloem traces moving from the roots into the stem. Since Alexa-Histone was not recovered in the apoplastic wash fluid, but the Alexa-Histone fluorescence intensity level is still higher than Alexa-BSA, which can be found in both apoplast and symplast. It is notable that petiole cross sections show Alexa-Histone was unload from the phloem into neighboring cell layers. This exterior phloem transport maybe affects the pressure gradient within the sieve tube and increasing the uptake of Alexa-Histone. After

the first uptake phase of Alexa-Histone, the fluorescence intensity of hydroponic plants petioles dropped, which suggests that water potential is not the driving force for Alexa-Histone movement.

It was interesting to observe the lateral vascular bundle fluorescence in petioles. CF dye moved in both the central and lateral (adaxial) vascular bundles, while Alexa-BSA, -Histone, and Fluorescein-HCV were mainly in the central vascular bundle. These data suggest that the adaxial vascular bundles are mainly used to transport solutes and not proteins. The adaxial position of the cottonwood lateral veins are connected to specific veins of the middle and bottom parts of leaf lamina, but there is very little known about the vascular continuity between the petiole and leaf lamina in *Nicotiana* ssp (Maksymowych, Orkwiszewski, and Maksymowych, 1983). More research is needed to know if they differ in their capacity for photoassimilate or protein transport.

The different fluorescence intensities between petiole and stem cross sections show that flow from the stem to leaves is regulated by petioles (Fig. 7 and 8). Panel c and d of Fig. 7 and 8 tell that the amount of fluorescence per mm^3 in the stem vascular rays is higher than in the leaf petioles. If there was a seamless transition during these vascular rays branching into the petioles, similar intensities would be shown. There might be a change in phloem strands dimension that transition from the stem into petioles and this controls the amount of proteins that enter or exit the petiole. The existence of a regulatory mechanism used to sort proteins to different destinations might be another explanation.

Although fluorescence intensity level of petiole cross sections in Alexa-BSA treated plant was low, MRI data show detectable movement of Alexa-BSA in *N.*

benthamiana vascular, and the transport rate can be quantified. MRI technology is widely used for studying vascular transport in mammalian systems and has been employed in few plant biology studies to describe flow dynamics as well as anatomical structures (Scheenen et al., 2002; Scheenen et al., 2007; Windt et al., 2006). MRI has been used for studying the long distance water transport in cucumber plants under normal and environmental stress conditions. Heavy water and gadolinium have been loaded into the vasculature as MRI tracers to quantify the flow velocities in Pharbitis nil (morning glory) (Gussoni et al., 2001). The velocity measures show significant rates of transport near the loading site, and as the ROIs move further away the rates drop. MRI results show rate of Gd-BSA movement (0.057 mm/s) in stem is slower than Gd-DTPA (0.077 mm/s), which is concordant with fluorescence images and imageJ data. This lends measuring fluorescence intensities in cross sections over time as a credible approach to study protein movement in vascular. While MRI measures signal intensities in digital ROIs, cross sections were employed as ROIs and fluorescence levels were measured directly in the vasculature tissues. MRI technology is powerful but expensive and so the ability to obtain valuable profiles of protein movement through the phloem provides a cheaper and useful alternative to studying protein mobility in the phloem.

The unloading pattern of CF dye and fluorescent proteins were also investigated in this research, the intensities are adequate to detect in leaf veins and lamina during 90 min post-delivery (Fig. 10 and 11). It was interesting to see the unloading patterns for Alexa-BSA, -Histone, and Fluorescein-HCV were unique to each of the proteins and they did not display the same pattern as CF dye for movement into minor veins, or unloading to the mesophyll. CF dye is an indicator used to differentiate sink, source/sink transition,

and source leaves (Roberts *et al.*, 1997). In sink leaves, CF dye entered major and minor veins, and can bleed into surrounding tissues, mainly from major veins. The fluorescent spots on the leaf lamina images of Alexa-BSA and Alexa-Histone treated plants exhibit the complete unloading pattern. There were minimal proteins left in small regions of the leaf veins. Fluorescence was prominent in the epidermal and mesophyll cells (fluorescent spots) and on rare occasions some fluorescence highlighted major veins (Fig. 10). Therefore, regardless of the protein dimensions and the intensity of fluorescence in distal parts of the plant, no obvious barrier preventing extensive movement of exogenous proteins were shown within the vasculature. The fact that both proteins were largely removed from the veins suggests that there is a mechanism sort proteins associated with leaf veins and clears exogenous proteins. Such mechanism might be related to defense mechanism, operating to reduce the level of toxic or foreign proteins in the plant vascular system.

The unloading pattern of Fluorescein-HCV core protein is especially interesting that it was similar to CF dye. Fluorescein-HCV resided mainly in major and minor veins in sink leaves and did not show neighboring cells fluorescence during 90 min. This pattern of movement is unlike the other exogenous proteins. There are numerous reports that indicate plant viruses or capsid proteins are restricted to the phloem and can only unload with the help of viral movement protein (Mekuria et al., 2008; Roberts et al., 1997; Silva et al., 2002). These data suggest that there is a mechanism in plants that specifically regulates viral proteins in the phloem. Once the virus core protein is loaded into the phloem it can then spread throughout the plant vasculature. The restriction of protein unloading can be used as defense mechanism limiting virus spread. Or whether

proteins complete vascular unloading, as for BSA and Histone, represents a defense mechanism that clears foreign proteins from the plant vasculature. However the contrasting data raises intriguing questions for future research.

B. oleracea plants were used in this study because they have a different arrangement of vascular bundles in petioles to investigate the influence of bundle arrangement to the quality of mass flow. And as a common vegetable, *B. oleracea* exhibit what kind of response when the exogenous proteins loaded into plants might contribute to the study of disease outbreak related to contaminated groundwater in the field. CF dye (460 Da), Alexa-Histone (34 kDa), Alexa-BSA (66 kDa) were applied to *B. oleracea* plants to study their movement from the loading site to upper leaves. Since *B. oleracea* has two classes of vascular bundles in the petiole, which are large fan-shaped bundles and smaller circular bundles. It was intriguing to know what different function they perform during protein transport. The fluorescence intensity of L5 petiole show equal distribution of CF dye among fan shaped and circular bundles, while the transport capability of fan shaped and circular bundles differ when Alexa-BSA or -Histone were loaded into *B. oleracea.* Alexa-BSA was mainly present in the xylem strands of fan shaped bundles, while the circular bundles exhibit weaker fluorescence than fan shaped bundles. As for Alexa-Histone, the fluorescence spread throughout whole fans shaped bundles, but circular bundles only gain low level of fluorescence intensity. These data indicate fan shaped and circular bundles have similar capability when transfer solution like CF dye, but when it comes to the proteins, the function of two kinds of bundles might be different.

When comparing the transport ability of L5 petioles between *N. benthamiana* and *B. oleracea*, it is found that although the average fluorescence intensity per mm^3 of *B.*

oleracea L5 petiole vascular bundles are lower than in *N. benthamiana*, the total intensity levels per cross section of *B. oleracea* L5 petiole are higher, since *B. oleracea* plants have at least 5 vascular bundles per cross section (Fig. 14 and Table 5). The uptake of Alexa-BSA in *N. benthamiana* show 0.6-0.8 $\times 10^5$ FU mm^{-3} following L1 petiole application and 4.2-5.5 $\times 10^5$ FU mm^{-3} following root application, while in *B. oleracea* are only 0-0.7 $\times 10^5$ FU mm^{-3} following L1 petiole application and 0.2-3.1 $\times 10^5$ FU mm^{-3} following root application. But after calculate the total fluorescence unit uptake per cross section between *B. oleracea* and *N.benthamiana*, it is noticed that *B. oleracea* uptake more BSA than *N.benthamiana* (0.2-0.3 $\times 10^4$ FU following L1 petiole application and 0.1-1.4 $\times 10^4$ FU following root application in *N. benthamiana*, while in *B. oleracea* the numbers are 0-1.1 $\times 10^4$ FU following L1 petiole application and 0.3-5.2 $\times 10^4$ FU following root application (Table 5). This is also true for Alexa-Histone and the transport of CF dye at 90 min.

Table 5. Comparison of average of sum fluorescence units per L5 petiole cross section between *B. oleracea* and *N.benthamiana.* ($\times 10^4$ FU)

Broccoli L5 petiole						
Time (min)	Soil grown-L1 petiole application			Soil grown-root application		
	CF dye	BSA	Histone	CF dye	BSA	Histone
10	0.0 ±0.0	0.1 ±0.0	0.3 ±0.0	2.0 ±0.1	0.3 ±0.1	1.1 ±0.1
30	0.0 ±0.0	0.0 ±0.1	0.2 ±0.1	4.7 ±1.1	1.5 ±0.2	4.2 ±0.2
60	0.0 ±0.0	0.8 ±0.0	0.2 ±0.0	6.7 ±0.1	0.8 ±0.0	4.1 ±0.2
90	12.4 ±0.2	1.1 ±0.2	0.2 ±0.0	9.4 ±1.0	5.2 ±0.1	4.4 ±0.1
N. benthamiana L5 petiole						
Time (min)	Soil grown-L1 petiole application			Soil grown-root application		
	CF dye	BSA	Histone	CF dye	BSA	Histone
10	0.8 ±0.0	0.2 ±0.1	0.1 ±0.0	0.5 ±0.2	0.1 ±0.0	1.1 ±0.3
30	1.3 ±0.1	0.3 ±0.0	0.2 ±0.1	4.0 ±0.9	0.6 ±0.1	1.0 ±0.5
60	3.2 ±0.1	0.3 ±0.1	0.2 ±0.1	3.0 ±0.4	0.3 ±0.1	4.8 ±0.2
90	1.5 ±0.1	0.2 ±0.0	0.0 ±0.0	5.8 ±0.3	1.4 ±0.2	2.9 ±0.2

The summary of fluorescence intensities in all petioles of *B. oleracea* plants reveals that although the phenomenon that higher level of FU in same orthostichy side distribution of CF dye and fluorescent proteins occur in *N. benthamiana*, it never happened in *B. oleracea*. The movement of CF dye and proteins shows higher level of FU in the petioles near loading site when they were applied to L1 petiole in soil grown plants.

The transport level of Alexa-Histone was lower than its transfer in *N. benthamiana*. Although the size of protein does not affect the first uptake phase in *N. benthamiana*, it decreased the uptake of Alexa-Histone in first 10 min in *B. oleracea*. It is interesting that the hydroponic system can generally increase the fluorescence intensity of CF and proteins no matter the application methods. In addition, the hydroponic medium also contributes to the equal distribution of CF and proteins in all petioles following root application, which is presented by the overlapping of petioles FU lines in Fig. 16a. These indicate the factors which influence the fluorescence distribution in different plants are different.

The unloading pattern of Alexa-BSA and -Histone is unique from CF dye. In *B. oleracea* plants, the CF dye still unloaded from minor veins and show bleeding pattern like in *N. benthamiana*. While the unloading of Alexa-BSA and -Histone was from *B. oleracea* stomata, which is different from the epidermal and mesophyll fluorescence spots in *N. benthamiana*. The stomata unloading in *B. oleracea* is not a complete unloading form since there are still amount of fluorescence left in veins. But this unique unloading form from *N. benthamiana* indicates the different mechanism of expelling exogenous proteins in different plants.

Researchers have reported enteric viruses and hepatitis A are common in vegetables and that contaminated groundwater could be a source for viral outbreaks. These contaminating viruses have been identified using diagnostic criteria and have not fully investigated the penetrance of the viruses into internal tissues. Evidence of HCV core in the *N. benthamiana* vasculature sheds new light on the potential uptake of foodborne contaminants by plants. These data and the protein movement research in *N. benthamiana* and *B. oleracea* might be used to lay a foundation to study foodborne contaminants by plants. A single viral protein can easily be taken up by an edible plant just by loading the proteins to roots or petioles. This could be a source of edible vaccines that has never been tested. In addition, these data suggest that exogenous proteins, including viral proteins, can follow the flow of assimilates throughout the plant but there is a mechanism that differentiates foreign proteins for transport to the apoplast, unloading to leaf lamina, or restriction to leaf veins.

REFERENCES

Agrios, G. N. (1969). "Plant pathology." Academic Press, New York,.

Avery, G. S. (1933). Structure and development of the tobacco leaf. *Am. J. Bot.* **20,** 565-592.

Balachandran, S., Xiang, Y., Schobert, C., Thompson, G. A., and Lucas, W. J. (1997). Phloem sap proteins from Cucurbita maxima and Ricinus communis have the capacity to traffic cell to cell through plasmodesmata. *Proc Natl Acad Sci U S A* **94**(25)**,** 14150-5.

Baumert, T. F., Ito, S., Wong, D. T., and Liang, T. J. (1998). Hepatitis C virus structural proteins assemble into viruslike particles in insect cells. *J Virol* **72**(5)**,** 3827-36.

Bokman, S. H., and Ward, W. W. (1981). Renaturation of Aequorea gree-fluorescent protein. *Biochem Biophys Res Commun* **101**(4)**,** 1372-80.

Buhtz, A., Springer, F., Chappell, L., Baulcombe, D. C., and Kehr, J. (2008). Identification and characterization of small RNAs from the phloem of Brassica napus. *Plant J* **53**(5)**,** 739-49.

Carrington, J. C., Kasschau, K. D., Mahajan, S. K., and Schaad, M. C. (1996). Cell-to-cell and long-distance transport of viruses in plants. *Plant Cell* **8,** 1669-1681.

Carrington, J. C., and Whitham, S. A. (1998). Viral invasion and host defense: strategies and counter-strategies. *Curr Opin Plant Biol* **1**(4)**,** 336-41.

Choo, Q. L., Kuo, G., Weiner, A. J., Overby, L. R., Bradley, D. W., and Houghton, M. (1989). Isolation of a cDNA clone derived from a blood-borne non-A, non-B viral hepatitis genome. *Science* **244**(4902)**,** 359-62.

Ding, B., Parthasarathy, M. V., Niklas, K., and Turgeon, R. (1988). A morphometric analysis of the phloem-unloading pathway in developing tobacco leaves. *Planta* **176,** 307-318.

Donker, H. C., and Van As, H. (1999). Cell water balance of white button mushrooms (Agaricus bisporus) during its post-harvest lifetime studied by quantitative magnetic resonance imaging. *Biochim Biophys Acta* **1427**(2)**,** 287-97.

Esau, K. (1975). "Plant Anatomy." 2nd ed. John Wiley & Sons, Inc., New York.

Giakountis, A., and Coupland, G. (2008). Phloem transport of flowering signals. *Curr Opin Plant Biol* **11**(6)**,** 687-94.

Giavalisco, P., Kapitza, K., Kolasa, A., Buhtz, A., and Kehr, J. (2006). Towards the proteome of Brassica napus phloem sap. *Proteomics* **6**(3)**,** 896-909.

Golecki, B., Schulz, A., and Thompson, G. A. (1999). Translocation of structural P proteins in the phloem. *Plant Cell* **11**(1)**,** 127-40.

Grignon, N., Touraine, B., and Durand, M. (1989). 6(5)Carboxyfluorescein as a tracer of phloem sap translocation. *Amer. J. Bot.* **76,** 871-877.

Guo, L., Yu, Y., Xia, X., and Yin, W. (2010). Identification and functional characterisation of the promoter of the calcium sensor gene CBL1 from the xerophyte Ammopiptanthus mongolicus. *BMC Plant Biol* **10,** 18.

Gussoni, M., Greco, F., Vezzoli, A., Osuga, T., and Zetta, L. (2001). Magnetic resonance imaging of molecular transport in living morning glory stems. *Magn Reson Imaging* **19**(10)**,** 1311-22.

Hall, S., and Baker, D. (1972). The chemical composition of Ricinus phloem exudate. *Planta (Berl.)* **106,** 131-140.

Imlau, A., Truernit, E., and Sauer, N. (1999). Cell-to-cell and long-distance trafficking of the green fluorescent protein in the phloem and symplastic unloading of the protein into sink tissues. *Plant Cell* **11**(3)**,** 309-22.

Joy, K. W. (1964). Translocation in Sugar-Beet .I. Assimilation of 14co2 + Distribution of Materials from Leaves. *Journal of Experimental Botany* **15**(45)**,** 485-&.

Lewis, J. D., Destito, G., Zijlstra, A., Gonzalez, M. J., Quigley, J. P., Manchester, M., and Stuhlmann, H. (2006). Viral nanoparticles as tools for intravital vascular imaging. *Nat Med* **12**(3)**,** 354-60.

Li, Y., Fuchs, M., Cohen, S., Cohen, Y., and Wallach, R. (2002). Water uptake profile response of corn to soil moisture depletion. *Plant Cell and Environment* **25**(4)**,** 491-500.

Loo, L., Guenther, R. H., Lommel, S. A., and Franzen, S. (2007). Encapsidation of nanoparticles by red clover necrotic mosaic virus. *J Am Chem Soc* **129**(36)**,** 11111-7.

Loo, L., Guenther, R. H., Lommel, S. A., and Franzen, S. (2008). Infusion of dye molecules into Red clover necrotic mosaic virus. *Chem Commun (Camb)*(1)**,** 88-90.

Lucas, W. J., and Wolf, S. (1999). Connections between virus movement, macromolecular signaling and assimilate allocation. *Curr Opin Plant Biol* **2**(3)**,** 192-7.

Maksymowych, A. B., Orkwiszewski, J. A. J., and Maksymowych, R. (1983). Vascular Bundles in Petioles of Some Herbaceous and Woody Dicotyledons. *American Journal of Botany* **70**(9)**,** 1289-1296.

Manchester, M., and Singh, P. (2006). Virus-based nanoparticles (VNPs): platform technologies for diagnostic imaging. *Adv Drug Deliv Rev* **58**(14)**,** 1505-22.

Maniatis, T., Fritsch, E. F., and Sambrook, J. (1982). "Molecular cloning : a laboratory manual." Cold Spring Harbor Laboratory, Cold Spring Harbor, N.Y.

Mekuria, T., Bamunusinghe, D., Payton, M., and Verchot-Lubicz, J. (2008). Phloem unloading of potato virus X movement proteins is regulated by virus and host factors. *Mol Plant Microbe Interact* **21**(8)**,** 1106-17.

Metcalfe, C., and Chalk, L. (1979). "Anatomy of the dicotyledons." 1st ed., Volume 1 Clarendon Press, Oxford.

Moriya, K., Yotsuyanagi, H., Shintani, Y., Fujie, H., Ishibashi, K., Matsuura, Y., Miyamura, T., and Koike, K. (1997). Hepatitis C virus core protein induces hepatic steatosis in transgenic mice. *J Gen Virol* **78 (Pt 7),** 1527-31.

Nelson, T., and Dengler, N. (1997). Leaf vascular pattern formation. *Plant Cell* **9,** 1121-1135.

Oparka, K. J., and Turgeon, R. (1999). Sieve elements and companion cells-traffic control centers of the phloem. *Plant Cell* **11**(4)**,** 739-50.

Ormö, M., Cubitt, A. B., Kallio, K., Gross, L. A., Tsien, R. Y., and Remington, S. J. (1996). Crystal structure of the *Aequorea victoria* green fluorescent protein. *Science* **273,** 1392–1395.

Osuga, T., Obata, T., Ikehira, H., Tanada, S., Sasaki, Y., and Naito, H. (1998). Dialysate pressure isobars in a hollow-fiber dialyzer determined from magnetic resonance imaging and numerical simulation of dialysate flow. *Artif Organs* **22**(10)**,** 907-9.

Roberts, A. G., Cruz, S. S., Roberts, I. M., Prior, D., Turgeon, R., and Oparka, K. J. (1997). Phloem Unloading in Sink Leaves of Nicotiana benthamiana: Comparison of a Fluorescent Solute with a Fluorescent Virus. *Plant Cell* **9**(8)**,** 1381-1396.

Saito, I., Miyamura, T., Ohbayashi, A., Harada, H., Katayama, T., Kikuchi, S., Watanabe, Y., Koi, S., Onji, M., Ohta, Y., Choo, Q. L., Houghton, M., and Kuo, G. (1990). Hepatitis-C Virus-Infection Is Associated with the Development of Hepatocellular-Carcinoma. *Proceedings of the National Academy of Sciences of the United States of America* **87**(17)**,** 6547-6549.

Santolini, E., Migliaccio, G., and La Monica, N. (1994). Biosynthesis and biochemical properties of the hepatitis C virus core protein. *J Virol* **68**(6)**,** 3631-41.

Sapsford, K. E., Soto, C. M., Blum, A. S., Chatterji, A., Lin, T., Johnson, J. E., Ligler, F. S., and Ratna, B. R. (2006). A cowpea mosaic virus nanoscaffold for multiplexed antibody conjugation: application as an immunoassay tracer. *Biosens Bioelectron* **21**(8)**,** 1668-73.

Scheenen, T., Heemskerk, A., de Jager, A., Vergeldt, F., and Van As, H. (2002). Functional imaging of plants: a nuclear magnetic resonance study of a cucumber plant. *Biophys J* **82**(1 Pt 1)**,** 481-92.

Scheenen, T. W., Vergeldt, F. J., Heemskerk, A. M., and Van As, H. (2007). Intact plant magnetic resonance imaging to study dynamics in long-distance sap flow and flow-conducting surface area. *Plant Physiol* **144**(2)**,** 1157-65.

Shih, C. M., Lo, S. J., Miyamura, T., Chen, S. Y., and Lee, Y. H. (1993). Suppression of hepatitis B virus expression and replication by hepatitis C virus core protein in HuH-7 cells. *J Virol* **67**(10)**,** 5823-32.

Silva, M. S., Wellink, J., Goldbach, R. W., and van Lent, J. W. (2002). Phloem loading and unloading of Cowpea mosaic virus in Vigna unguiculata. *J Gen Virol* **83**(Pt 6)**,** 1493-504.

Song, H., Li, J., Shi, S., Yan, L., Zhuang, H., and Li, K. (2010). Thermal stability and inactivation of hepatitis C virus grown in cell culture. *Virol J* **7,** 40.

Suzuki, R., Matsuura, Y., Suzuki, T., Ando, A., Chiba, J., Harada, S., Saito, I., and Miyamura, T. (1995). Nuclear localization of the truncated hepatitis C virus core protein with its hydrophobic C terminus deleted. *J Gen Virol* **76 (Pt 1),** 53-61.

Taiz, L., and Zeiger, E., Eds. (2006). Plant Physiology. 4th ed. Sunderlad MA: SInauer Assoc.

Towner, R. A., Smith, N., Doblas, S., Tesiram, Y., Garteiser, P., Saunders, D., Cranford, R., Silasi-Mansat, R., Herlea, O., Ivanciu, L., Wu, D., and Lupu, F. (2008). In vivo detection of c-Met expression in a rat C6 glioma model. *J Cell Mol Med* **12**(1)**,** 174-86.

Van Lent, J., Storms, M. and Goldbach, R. (1990). Evidence for the involvement of 58K and 48K proteins in the intercellular movement of cowpea mosaic virus. *Journal of General Virology* **71,** 219-223.

Van Lent, J., Storms, M., Van Der Meer, F., Wellink, J. and Goldbach, R. (1991). Tubular structures involved in movement of cowpea mosaic virus are also formed in infected protoplasts. *Journal of General Virology* **72,** 2615-2623.

Windt, C. W., Vergeldt, F. J., de Jager, P. A., and van As, H. (2006). MRI of long-distance water transport: a comparison of the phloem and xylem flow characteristics and dynamics in poplar, castor bean, tomato and tobacco. *Plant Cell Environ* **29**(9)**,** 1715-29.

Wolf, S., Deom, C.M., Beachy, R.N., and Lucas, W.J. (1989). Movement protein of tobacco mosaic virus modifies plasmodesmata size exclusion limit. *Science* **246,** 377–379.

Yang, Y., Ding, B., Baulcombe, D. C., and Verchot, J. (2000). Cell-to-cell movement of the 25K protein of potato virus X is regulated by three other viral proteins. *Mol Plant Microbe Interact* **13**(6)**,** 599-605.

VITA

CHENXING NIU

Candidate for the Degree of

Master of Science

Thesis: A STUDY OF VASCULAR TRANSPORT OF PLANT EXOGENOUS PROTEINS IN *NICOTIANA BENTHAMIANA* AND *BRASSICA OLERACEA* USING FLUORESCENCE AND MEGNETIC RESONANCE IMAGING TECHNOLOGY

Major Field: Plant Pathology

Biographical:

Personal Data: Born in Beijing, China on July 31, 1986, the daughter of Xiaopu Zhou and Tao Niu.

Education: Received Bachelor of Science degree in Agronomy, majored in Plant Protection from China Agricultural University, Beijing, China. Completed the requirements for the Master of Science in Plant Pathology at Oklahoma State University, Stillwater, Oklahoma in July, 2011.

Experience:

Graduate Research Assistant, Department of Entomology and Plant Pathology, Oklahoma State University, Stillwater, OK, August 2009 to July 2011.

Narrator, China Science and Technology Museum, January 2008 to February 2008.

Name: Chenxing Niu Date of Degree: July, 2011

Institution: Oklahoma State University Location: Stillwater, Oklahoma

Title of Study: A STUDY OF VASCULAR TRANSPORT OF PLANT EXOGENOUS PROTEINS IN *NICOTIANA BENTHAMIANA* AND *BRASSICA OLERACEA* USING FLUORESCENCE AND MEGNETIC RESONANCE IMAGING TECHNOLOGY

Pages in Study: 101 Candidate for the Degree of Master of Science

Major Field: Plant Pathology

Scope and Method of Study:

Use fluorescence and MRI imaging technology to characterize long distance transport of fluorescence conjugated proteins and virus protein in *Nicotiana benthamiana* and *Brassica oleracea*. The investigation of vascular transport of exogenously applied proteins will lay the foundation of studying the movement of virion nanoparticles as biomedicine in plants and help to study potential uptake of foodborne contaminants by plants.

Findings and Conclusions:

Research on the vascular transport of exogenously applied proteins and compared their delivery to various parts of the *Nicotiana benthamiana* and *Brassica oleracea* plants with carboxy fluorescein dye reveals Alexa fluor tagged bovine serum albumin (Alexa-BSA) follows a low level of movement to upper parts of the plant and unloads to the apoplast. Alexa fluor tagged Histone H1 (Alexa-Histone) moves relatively rapid and is retained in the phloem and phloem parenchyma. Both Alexa-Histone and -BSA were exported from leaf veins class II and III but they unloaded completely into the leaf lamina as fluorescent epidermal and mesophyll cells in *N. benthamiana* and as fluorescent stomata in *B. oleracea*. There is barely any residual fluorescence left inside the leaf veins in *N. benthamiana*. Fluorescein tagged hepatitis C virus core protein (fluorescein-HCV) moves more rapidly than BSA in *N. benthamiana* but does not reach the level of Histone through the plant and was restricted to the leaf veins. Fluorescein-HCV failed to unload to the leaf lamina. These combined data suggest that there is not a single default pathway for the transfer of exogenous proteins through the plant. Specific protein properties appear to determine their destination and transport properties within the phloem. The factors of water content, application methods play different roles on protein transport in different plants.

ADVISER'S APPROVAL: Dr. Jeanmarie Verchot